

Consensus-Based Peer-to-Peer Control Architecture for Multiuser Haptic Interaction Over the Internet

Ke Huang and Dongjun Lee, *Member, IEEE*

Abstract—We propose a novel peer-to-peer (P2P) distributed control architecture for the shared haptic interaction among remotely located users over partially connected and undirected unreliable Internet communication network with varying delay, packet loss, data swapping/duplication, etc. Each user simulates and interacts with their own local copy of the shared deformable virtual object (for haptic responsiveness against latency), while these local copies are synchronized via a proportional-derivative type consensus control over the Internet communication network (for haptic experience consistency among the users). Our proposed architecture enforces passivity, thereby, rendering itself to be interaction stable, portable, and scalable for heterogeneous (passive) users and devices. Configuration consensus among the local copies and force balance among the users are also shown. The issue of optimizing communication network topology is also addressed with some relevant experimental results.

Index Terms—Communication graph, consensus, Internet, multiuser shared haptic interaction, passivity.

I. INTRODUCTION

MULTIUSER shared haptic interaction among remotely located users over the Internet would enable many powerful applications: virtual collaborative surgical training, collaborative haptic evaluation of computer-aided designs, virtual sculpting among remote artists, and haptically enabled networked computer games, to name just few. Perhaps, even more importantly, this idea of multiuser haptic interaction over the Internet may also revolutionize our way of interacting with each other in the cyberspace, by complementing currently available virtual-reality vision and audio interaction modalities (see Fig. 1).

In this paper, extending our recent results of [1]–[3], we propose a novel peer-to-peer (P2P) control architecture for this problem, as depicted in Fig. 2, which can be summarized as follows. First, to achieve real-time *responsiveness* of haptic feedback against the Internet’s latency, all N users simulate and

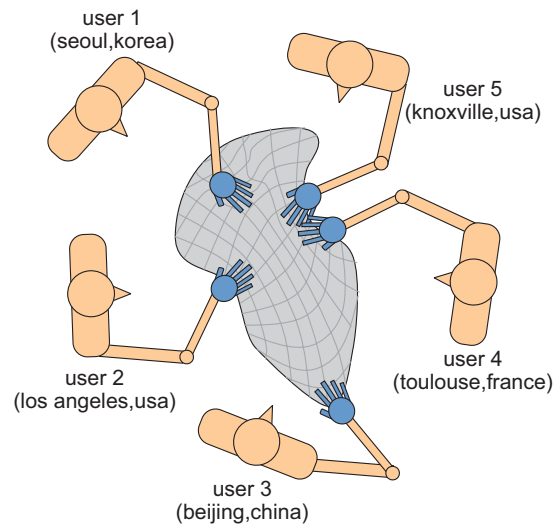


Fig. 1. Multiuser shared haptic interaction over the Internet.

interact with their own local copy (or replica) of a common shared deformable virtual object (VO). We then connect these N VO local copies’ configuration via a (discrete-time) proportional-derivative (PD) type consensus control (with some local damping injection) over the Internet to provide *consistency* of haptic experience among the distributed users. For this paper, we particularly focus on deformable VOs (e.g., surgical simulation [4]; see Fig. 1), which define a very useful, yet, quite challenging, class of haptic virtual environments. We also allow *general* unreliabilities for the Internet communication (e.g., varying delay, packet loss, data swapping, etc.), as well as assume that the communication topology among the N users over the Internet is only partially connected and undirected (i.e., if i th user receives data from j th user, so does j th user from i th user).

It is then well known that such a PD-type consensus coupling, which is established over the imperfect Internet, can easily become unstable. The issue of stability is even more challenging here, since our P2P architecture in Fig. 2 needs to be mechanically coupled with a wide range of heterogeneous, uncertain, unknown, and/or complicated human users and haptic devices. To address this issue of interaction stability, we enforce discrete-time N -port (closed-loop) passivity of our P2P architecture of Fig. 2. More precisely, 1) we adopt noniterative variable-rate passive mechanical integrators (NPMIs) [5], [6] to passively simulate each VO local copy in Fig. 2; and 2) we extend our recent results of [1]–[3] to guarantee N -port (controller) passivity of the PD-type consensus control loop (i.e., inner part of Fig. 2) over the unreliable and only partially connected (undirected)

Manuscript received July 24, 2012; accepted November 15, 2012. Date of publication December 20, 2012; date of current version April 1, 2013. This paper was recommended for publication by Associate Editor T. Asfour and Editor W. K. Chung upon evaluation of the reviewers’ comments. This work was supported in part by the U.S. National Science Foundation under CAREER Award IIS-0844890 and the Global Frontier R&D Program on Human-centered Interaction for Coexistence of the National Research Foundation funded by the Ministry of Education, Science, and Technology of Korea (NRF-M1AXA003-2011-0028355).

K. Huang is with Western Digital Corporation, Irvine, CA 92612 USA (e-mail: dahuang8@gmail.com).

D. J. Lee is with the School of Mechanical and Aerospace Engineering and Institute of Advanced Machinery and Design, Seoul National University, Seoul 151-744, Korea (e-mail: djlee@snu.ac.kr).

Color versions of one or more of the figures in this paper are available online at <http://ieeexplore.ieee.org>.

Digital Object Identifier 10.1109/TRO.2012.2229672

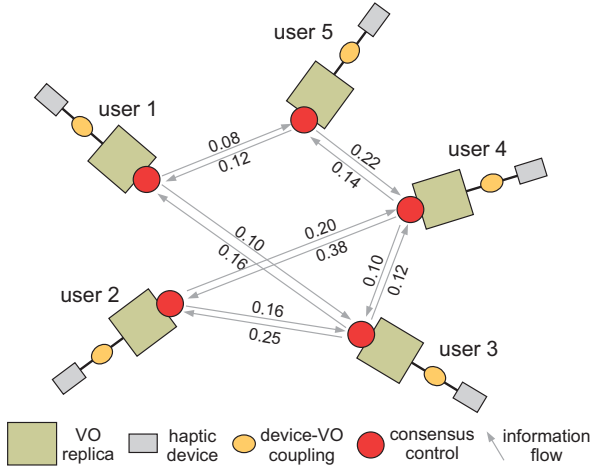


Fig. 2. P2P multiuser haptic interaction architecture.

Internet communication network with varying delay, packet loss, data swapping, etc.

This discrete-time N -port (closed-loop) passivity then endows our P2P architecture with the following useful/powerful properties.

1) *Interaction stability*: With some passive (hybrid) device-VO coupling for Fig. 2 (e.g., virtual coupling [7], [8], or passive set-position modulation (PSPM) [9]), we can enforce interaction stability with *any* human user and haptic device, regardless of however heterogeneous, uncertain, unknown, or complicated they are, as long as they are, or behave as, passive systems [10], [11].

2) *Portability*: The design of shared VO and consensus control can be done independently from the physical construction and properties of haptic devices (i.e., device-simulation separation [12]), implying that we can deploy *any* (passive) devices, while keeping the same VO and consensus coupling (e.g., no need to increase shared VO's mass for all users even if new devices' damping is deficient [13]).

3) *Scalability*: Since the aforementioned properties hold for any number of (passive) users/devices, our P2P architecture, with its own distributed nature, can accommodate *any* number of users/devices.

Some results and frameworks have been reported for the problem of multiuser shared haptic interaction over the Internet. However, most of them are rather empirical and qualitative (e.g., [14]–[21]), without (often useful and important) theoretical guarantees of stability or performance. The work of [22] and [23] may be considered as exceptions. Yet, some of the important aspects/issues of the multiuser shared haptic interaction, which are fully incorporated in this paper, were not considered there (e.g., unknown nonlinear heterogeneous users/devices, varying delay and packet loss, arbitrary network topology, portability and scalability, etc.). To our knowledge, our P2P control architecture, which is presented in this paper, is the very first result for multiuser shared haptic interaction via a common (nontrivial) deformable VO over the unreliable and partially connected (discrete) Internet communication network with theoretical guarantees of passivity and (steady-state) performance.

One of the key building blocks of our P2P architecture is the consensus control among the N discrete-time second-order VO local copies over the unreliable and partially connected Internet network. Some results have been proposed for this problem (e.g., [24]–[26]); yet, to our knowledge, none of them either utilizes or achieves passivity, which is crucial for our P2P architecture, as mentioned previously. In addition to this passivity property, our PD-based consensus result can also handle the following issues altogether unlike other consensus techniques: nonuniform varying delay and packet loss (unlike, e.g., [24] and [25]); multidimensional consensus (unlike, e.g., [26]); and variable update rate (unlike, e.g., [24]–[26]). In this paper, we also extend the well-known 1-D Laplacian of undirected graphs [27]–[29] to the multidimensional case, where the weight on each edge is given by a symmetric and positive-definite matrix rather than a scalar (see Section II-B).

The rest of this paper is organized as follows. In Section II, we review basic graph theory and extend the scalar graph Laplacian to the multidimensional case. Our novel P2P architecture is presented and its properties are detailed in Section III, which consists of passive local VO simulation (Section III-A), passive VO consensus over the Internet (Section III-B), and passive device-VO coupling (Section III-C). The issue of network topology optimization is discussed in Section IV, and experimental results are presented in Section V. Concluding remarks and some comments on future research are given in Section VI.

Some preliminary results of this paper have been presented in [1], [2] (only for constant delay), and [3] (only for master-slave teleoperation). This paper extends the results of [1]–[3] to the multiuser shared haptic interaction over the unreliable and partially connected Internet networks with varying delay, packet loss, data swapping/duplication, etc., while also presenting new experimental results with a (nontrivial) 3-D deformable VO.

II. GRAPH THEORY

A. Basic Notations and Properties

We use graph theory [30] to describe the communication topology among the N users over the Internet. For this, we define $\mathcal{G}(\mathcal{V}, \mathcal{E})$ to be a graph where $\mathcal{V} := \{v_1, \dots, v_N\}$ and $\mathcal{E} \subseteq \mathcal{V} \times \mathcal{V}$ are, respectively, the set of N vertexes¹ (i.e., users or their VOs) and the set of N_e edges connecting them (i.e., information flow). Each directed edge of \mathcal{E} can then be identified either by e_{ij} with v_i and v_j being the head and tail of e_{ij} (e.g., v_i receives information from v_j) or by e_l with $l \in \mathcal{E}_C := \{1, 2, \dots, N_e\}$. In fact, we can define a bijective map between $l \in \mathcal{E}_C$ (i.e., *one-tuple* enumeration) and $(i, j) \in \mathcal{E}_P := \{(i, j) | e_{ij} \in \mathcal{E}, v_i, v_j \in \mathcal{V}\}$ (i.e., *two-tuple* enumeration). We will denote this equivalence between \mathcal{E}_P and \mathcal{E}_C by

$$l \approx (i, j) \quad \text{if } e_l = e_{ij} \in \mathcal{E}.$$

In this paper, we assume $\mathcal{G}(\mathcal{V}, \mathcal{E})$ is simple (i.e., no self-loops) and undirected (i.e., $e_{ij} \in \mathcal{E} \leftrightarrow e_{ji} \in \mathcal{E}$). We also define the information neighbors of v_i s.t.

$$\mathcal{N}_i := \{v_j \in \mathcal{V} | e_{ij} \in \mathcal{E}\}$$

¹We use the term vertexes to describe the communication graph $\mathcal{G}(\mathcal{V}, \mathcal{E})$, while the term nodes for the structure graph $\mathcal{G}_{VO}(\mathcal{X}, \mathcal{K})$ of the deformable VO in Section III-A.

i.e., the set of users from which v_i receives information. We will also use the following facts, whose proofs are omitted here due to their simplicity: For any $\varepsilon : \mathcal{E}_P \rightarrow \mathfrak{R}^m$

$$\sum_{i=1}^N \sum_{j \in \mathcal{N}_i} \varepsilon_{ij} = \sum_{l=1, (p,q) \approx l}^{N_e} \varepsilon_{pq} \quad (1)$$

and, further, if $\mathcal{G}(\mathcal{V}, \mathcal{E})$ is undirected

$$\sum_{l=1, (p,q) \approx l}^{N_e} \varepsilon_{pq} = \frac{1}{2} \sum_{l=1, (p,q) \approx l}^{N_e} (\varepsilon_{pq} + \varepsilon_{qp}). \quad (2)$$

For $\mathcal{G}(\mathcal{V}, \mathcal{E})$, the incidence matrix $\mathcal{D} := \{d_{il}\} \in \mathfrak{R}^{N \times N_e}$ is defined by

$$d_{il} := \begin{cases} 1, & \text{if } v_i \text{ is the head of } e_l \\ -1, & \text{if } v_i \text{ is the tail of } e_l \\ 0, & \text{otherwise} \end{cases} \quad (3)$$

and the graph Laplacian matrix $\mathcal{L} = \{l_{ij}\} \in \mathfrak{R}^{N \times N}$ by

$$l_{ij} := \begin{cases} \deg(v_i), & \text{if } i = j \\ -1, & \text{if } e_{ij} \in \mathcal{E} \\ 0, & \text{otherwise} \end{cases} \quad (4)$$

where $\deg(v_i)$ is the number of incoming edges of v_i . For undirected $\mathcal{G}(\mathcal{V}, \mathcal{E})$, we then have [30, Prop. 4.8]

$$\mathcal{L} = \mathcal{D}\mathcal{D}^T \quad (5)$$

and, moreover, if $\mathcal{G}(\mathcal{V}, \mathcal{E})$ is connected as well, \mathcal{L} has a zero eigenvalue at the origin with the eigenvector $\mathbf{1}_N := [1, \dots, 1]^T \in \mathfrak{R}^N$, and all the other eigenvalues are strictly positive real. See [27], [28], and [30] for more details.

B. Multidimensional Graph Laplacian: Stiffness Matrix \mathcal{P}

To attain consistency, our P2P architecture in Fig. 2 connects the N VO local copies via PD-type consensus control over $\mathcal{G}(\mathcal{V}, \mathcal{E})$. In contrast with the usual consensus results (e.g., [24]–[29]), here, we are interested in using n -dimensional (matrix) consensus gains $P_{ij} \in \mathfrak{R}^{n \times n}$ rather than 1-D (scalar) P_{ij} (i.e., $P_{ij} = p_{ij}I_n$, with a scalar $p_{ij} > 0$ and identity matrix $I_n \in \mathfrak{R}^{n \times n}$), where $n > 0$ is the dimension of the deformable VO configuration (see Section III-A). This is because 1) some nodes of the VO may need stronger consensus coupling than others (e.g., nodes with heavier mass); and 2) cross coupling among different nodes between two VOs may improve consensus performance [31].

Then, similar to \mathcal{L} in (4), we define the multidimensional graph Laplacian, or *stiffness matrix* $\mathcal{P} \in \mathfrak{R}^{nN \times nN}$, s.t.

$$P_{ij} = \begin{cases} \sum_{k \in \mathcal{N}_i} P_{ik}, & i = j \\ -P_{ij}, & i \neq j \text{ and } e_{ij} \in \mathcal{E} \\ 0, & \text{otherwise} \end{cases} \quad (6)$$

where $P_{ij} \in \mathfrak{R}^{n \times n}$ is the symmetric positive-definite consensus matrix gain on $e_{ij} \in \mathcal{E}$. To our knowledge, consensus property of \mathcal{P} has not been established. In the following, we show that \mathcal{P} indeed possesses consensus property similar to \mathcal{L} , thereby, extending the notion of 1-D Laplacian \mathcal{L} [27], [28] to multi-

dimensional stiffness matrix \mathcal{P} . For this, the following lemma is instrumental.

Lemma 1: Suppose that $\mathcal{G}(\mathcal{V}, \mathcal{E})$ is undirected, and P_{ij} in (6) is symmetric, positive definite, and $P_{ij} = P_{ji}$. Then, we can write the stiffness matrix \mathcal{P} in (6) s.t.

$$\mathcal{P} = \frac{1}{2} (\mathcal{D} \otimes I_n) P_d (\mathcal{D} \otimes I_n)^T \quad (7)$$

where $\mathcal{D} \in \mathfrak{R}^{N \times N_e}$ is the incidence matrix (3), \otimes is the Kronecker product, and $P_d := \text{diag}(P_1, P_2, \dots, P_{N_e}) \in \mathfrak{R}^{nN_e \times nN_e}$, with $P_l \in \mathfrak{R}^{n \times n}$ being the P-gain matrix assigned on $e_l \in \mathcal{E}$, $l \in \mathcal{E}_C = \{1, \dots, N_e\}$.

Proof: Define $\bar{D} := (\mathcal{D} \otimes I_n) P_d^{\frac{1}{2}} \in \mathfrak{R}^{nN \times nN_e}$. Then, its il th block matrix $\bar{d}_{il} \in \mathfrak{R}^{n \times n}$ is given by

$$\bar{d}_{il} = \begin{cases} P_l^{\frac{1}{2}}, & \text{if } v_i \text{ is the head of } e_l \\ -P_l^{\frac{1}{2}}, & \text{if } v_i \text{ is the tail of } e_l \\ 0, & \text{otherwise} \end{cases}$$

following the structure of \mathcal{D} in (3). Define also $\mathcal{E}_k := \{l \in \mathcal{E}_C \mid \exists v_r \in \mathcal{V} \text{ s.t. } l \approx (k, r) \text{ or } l \approx (r, k)\}$, i.e., the set of any edges connecting, or connected to, the vertex v_k . We then have $\bar{d}_{kl} = \pm P_l^{\frac{1}{2}} \neq 0$ if $l \in \mathcal{E}_k$, or $\bar{d}_{kl} = 0$ otherwise.

The $n \times n$ diagonal block of $\bar{D}\bar{D}^T$ is then given by

$$\sum_{l=1}^{N_e} \bar{d}_{il}^2 = \sum_{l \in \mathcal{E}_i} P_l = 2 \sum_{j \in \mathcal{N}_i} P_{ij}$$

for $i = 1, \dots, N$, since $\mathcal{G}(\mathcal{V}, \mathcal{E})$ is undirected, \mathcal{E}_i includes both the incoming and outgoing edges of v_i , and $P_{ji} = P_{ij}$. In addition, the $n \times n$ off-diagonal block of $\bar{D}\bar{D}^T$ is given by: $i, j \in \{1, 2, \dots, N\}$, $i \neq j$

$$\sum_{l=1}^{N_e} \bar{d}_{il} \bar{d}_{jl} = \sum_{l \in \mathcal{E}_i \cap \mathcal{E}_j} \bar{d}_{il} \bar{d}_{jl} = \sum_{l \approx (i,j), l \approx (j,i)} \bar{d}_{il} \bar{d}_{jl} = -2P_{ij}$$

since, with $i \neq j$, 1) if $l \notin \mathcal{E}_i \cap \mathcal{E}_j$, $\bar{d}_{il} \bar{d}_{jl} = 0$; 2) $l \in \mathcal{E}_i$ and $l \in \mathcal{E}_j$ implies that $l \approx (i, j)$ or $l \approx (j, i)$; and 3) $P_{ij} = P_{ji}$. This then shows that $2\mathcal{P} = \bar{D}\bar{D}^T$. ■

Using Lemma 1, we now show that the multidimensional stiffness matrix \mathcal{P} (6) indeed possesses consensus property similar to the 1-D (scalar) graph Laplacian \mathcal{L} (4).

Proposition 1: Suppose that $\mathcal{G}(\mathcal{V}, \mathcal{E})$ is undirected and connected, and $P_{ij} \in \mathfrak{R}^{n \times n}$ for (6) is symmetric, positive definite, and $P_{ij} = P_{ji}$. Then, we have

$$\text{rank}(\mathcal{P}) = n(N - 1)$$

with the n -dimensional kernel space of \mathcal{P} given by

$$\ker(\mathcal{P}) = \text{span}\{\mathbf{1}_N \otimes a_1, \dots, \mathbf{1}_N \otimes a_n\} \quad (8)$$

where $\text{span}\{a_1, a_2, \dots, a_n\} = \mathfrak{R}^n$.

Proof: Using Lemma 1, properties of rank and \otimes , and (5), with P_d being nonsingular, we have

$$\begin{aligned} \text{rank}(\mathcal{P}) &= \text{rank}((\mathcal{D} \otimes I_n) P_d^{\frac{1}{2}})^T [(\mathcal{D} \otimes I_n) P_d^{\frac{1}{2}}] \\ &= \text{rank}(P_d^{\frac{1}{2}} (\mathcal{D}^T \mathcal{D} \otimes I_n) P_d^{\frac{1}{2}}) \\ &= \text{rank}(I_n) \text{rank}(\mathcal{D}^T \mathcal{D}) = n \text{rank}(\mathcal{L}) \end{aligned}$$

where, if $\mathcal{G}(\mathcal{V}, \mathcal{E})$ is connected, $\text{rank}(\mathcal{L}) = N - 1$. Thus, we have $\text{rank}(\mathcal{P}) = n(N - 1)$, or equivalently, $\dim(\ker(\mathcal{P})) = n$. We can also verify that

$$\mathcal{P}(1_N \otimes a) = 0 \quad \forall a \in \mathbb{R}^n$$

which, with $\dim(\ker(\mathcal{P})) = n$, implies (8). ■

III. PEER-TO-PEER CONTROL ARCHITECTURE FOR MULTIUSER HAPTIC INTERACTION OVER THE INTERNET

We now present our novel P2P control architecture, as depicted in Fig. 2, which consists of the N local copies of the shared deformable VO, the consensus control among these N local copies over the Internet, and the local passive device–VO coupling. For this, we first utilize NPMI [5], [6] to render each VO local copy to be discrete-time passive (Section III-A). Then, extending our recent results of [2] and [3], we propose passivity-enforcing PD-type consensus control of the N local copies over the unreliable partially-connected and undirected Internet network with varying delay, packet loss, data swapping/duplication, etc. (Section III-B). Finally, even if it is a standard problem in haptics and not the main concern of this paper, for completeness, we briefly explain how to passively connect each VO local copy to a haptic device, particularly using the well-known virtual coupling technique [7], [8] (Section III-C).

A. Passive Local Simulation of Shared Virtual Object

We consider a linear deformable object as the shared VO. See Fig. 3 for an example. To enforce discrete-time passivity of this VO local simulation, we utilize our recently proposed NPMI [5], [6], which can be written as follows: For each i th user, $i = 1, \dots, N$

$$\begin{aligned} \frac{1}{N} [Ma_i(k) + B\hat{v}_i(k) + K(\hat{x}_i(k) - x_d)] &= \tau_i(k) + f_i(k) \\ a_i(k) &:= \frac{v_i(k+1) - v_i(k)}{T_i^k} \\ \hat{v}_i(k) &:= \frac{v_i(k+1) + v_i(k)}{2} = \frac{x_i(k+1) - x_i(k)}{T_i^k} \\ \hat{x}_i(k) &:= \frac{x_i(k+1) + x_i(k)}{2} \end{aligned} \quad (9)$$

where $k \geq 0$ is the discrete-time index; $T_i^k > 0$ is the integration interval; $x_i, v_i, a_i \in \mathbb{R}^{3n}$ are, respectively, the (combined) configuration, velocity, and acceleration of the n -nodes of the i th-user's VO (i.e., $x_i(k) := [x_i^1(k); x_i^2(k); \dots; x_i^n(k)]$, with $x_i^r(k) \in \mathbb{R}^3$ being the position of the VO's r th node: Similar also holds for v_i, a_i ; $x_d \in \mathbb{R}^{3n}$ specifies the VO's undeformed shape as well as its mechanical ground; $f_i(k) \in \mathbb{R}^{3n}$ is the device–VO interaction force (e.g., interaction with user-controlled virtual proxy: see Section III-C); and $\tau_i(k) \in \mathbb{R}^{3n}$ is to embed the consensus control for the N local copies over the Internet (see Section III-B).

In (9), $M \in \mathbb{R}^{3n \times 3n}$ is the symmetric positive-definite mass matrix of the n -nodes of VO; and $B, K \in \mathbb{R}^{3n \times 3n}$ are symmetric positive semidefinite (or definite) structural damping and spring matrices, typically decomposable by

$$B := B_{\text{int}} + B_{\text{gnd}}, \quad K := K_{\text{int}} + K_{\text{gnd}} \quad (10)$$



Fig. 3. Three-dimensional deformable VO, with 33 nodes, 87 tetrahedron meshes, and VP.

where \star_{int} defines internode coupling within the VO, while \star_{gnd} binds some nodes of VO to the mechanical ground x_d . More precisely, similar to (6), the 3×3 block matrix K_{int}^{rs} of $K_{\text{int}} \in \mathbb{R}^{3n \times 3n}$, $r, s \in \{1, 2, \dots, n\}$, is given by $K_{\text{int}}^{rs} := -K_{rs}$ if $r \neq s$; or $K_{\text{int}}^{rs} := \sum_{k \in \mathcal{N}_r^{\text{VO}}} K_{rk}$ if $r = s$, where $K_{rs} \in \mathbb{R}^{3 \times 3}$ is the spring gain between $x_i^r(k)$ and $x_i^s(k)$. On the other hand, K_{gnd} is given by $K_{\text{gnd}} := \text{diag}[k_{\text{gnd}}^1 I_3, \dots, k_{\text{gnd}}^n I_3]$, where $k_{\text{gnd}}^r > 0$ if the node x_i^r is attached to the mechanical ground x_d , or $k_{\text{gnd}}^r = 0$ otherwise.

Similar to the stiffness matrix \mathcal{P} in (6), $K_{\text{int}} \in \mathbb{R}^{3n \times 3n}$ then defines an undirected *structure graph* $\mathcal{G}_{\text{VO}}(\mathcal{X}, \mathcal{K})$, where $\mathcal{X} := \{x_i^1, x_i^2, \dots, x_i^n\}$ and $\mathcal{K} \in \mathcal{X} \times \mathcal{X}$, respectively, denote the VO's n -nodes and the K_{rs} -connections among them. Now, suppose that $K(x_i - x_d) \rightarrow 0$ in (9) and $\mathcal{G}_{\text{VO}}(\mathcal{X}, \mathcal{K})$ is connected. Then, from the structural similarity between \mathcal{P} and K_{int} (cf., Proposition 1), we will have 1) if $K_{\text{gnd}} = 0$

$$x_i - x_d \rightarrow \ker(K_{\text{int}}) \approx I_n \otimes z_i, \quad z_i \in \mathbb{R}^3$$

i.e., K_{int} enforces the VO to attain the undeformed shape x_d , whose location yet can “float” by an arbitrary displacement $z_i \in \mathbb{R}^3$ (i.e., symmetry in $E(3)$ [32]); and 2) if $K_{\text{gnd}} \neq 0$, $K = K_{\text{int}} + K_{\text{gnd}}$ becomes positive definite and $x_i \rightarrow x_d$ with $z_i = 0$ (i.e., symmetry breaking in $E(3)$ [32]). Similar can be said for B as well.

Since each user simulates the *shared* VO, the same M, B, K , and x_d are used in (9) for all users. We also assume that M, B, K , and x_d are all constant (see [6] for VO with varying M). Suppose also that the consensus among the N local copies is perfect with $x_i(k) \equiv x_j(k)$. Then, if a single user tries to deform its own VO local copy with all the other users not touching their copies, this user needs to make the same deformation across all the N local copies. This implies that the larger the number of VOs (i.e., N) is, the more difficult for each user to move/deform the (shared) VO. To address this scaling effect, similar to [1] and [20], we scale down (9) by N .

The NPMI algorithm (9) is implicit [i.e., $v_i(k+1), x_i(k+1), v_i(k), x_i(k)$ showing up together in the left-hand side of (9)], yet, still *noniterative*, i.e., if $\tau_i(k)$ and $f_i(k)$ are also given by a linear map of $\hat{v}_i(k), \hat{x}_i(k)$ and some exogenous signal $c_i(k) \in \mathbb{R}^p$ known at the onset of T_i^k , (9) can be reorganized s.t.

$$z_i(k+1) = H_k^i z_i(k) + G_k^i c_i(k) \quad (11)$$

where $z_i(k) := [v_i(k); x_i(k)] \in \mathbb{R}^{6n}$, $c_i(k) := [x_d; c_i(k)] \in \mathbb{R}^{3n+p}$, and $H_k^i \in \mathbb{R}^{3n \times 3n}$ and $G_k^i \in \mathbb{R}^{3n \times (3n+p)}$ are varying due to T_i^k contained in them. Equation (11) can then be solved without (typically time consuming) iterations, allowing us to

solve (9) haptically fast.² The NPMI VO model (9) may also be obtained via mass–spring–damper modeling [4] or finite element method [33].

The key property of NPMI, which is central for the construction of our P2P architecture, is that, unlike other integrators frequently used in haptics (e.g., explicit Euler [13]), it enforces (open-loop two-port) discrete-time passivity of (9). That is, using (9), we can easily show that $\forall \bar{M} \geq 0$

$$\sum_{k=0}^{\bar{M}} [f_i(k) + \tau_i(k)]^T \hat{v}_i(k) T_i^k \geq -E_i(0) =: -d_i^2 \quad (12)$$

where $E_i(k) := 1/N \times (\|v_i(k)\|_M^2/2 + \|x_i(k) - x_d\|_K^2/2)$ is the (scaled) total energy of the i th-user's VO, with $\|y\|_A := \sqrt{y^T A y}$ for a vector $y \in \mathfrak{R}^m$ and a positive definite/symmetric $A \in \mathfrak{R}^{m \times m}$. See [5] and [6] for more details on NPMI algorithm.

Now, let us define discrete-time N -port (closed-loop) passivity of the P2P architecture in Fig. 2: $\forall \bar{M} \geq 0, \exists d \in \mathfrak{R}, \text{ s.t.}$

$$\sum_{k=0}^{\bar{M}} \sum_{i=1}^N \hat{v}_i(k)^T f_i(k) T_i^k \geq -d^2 \quad (13)$$

i.e., maximum extractable energy from the N device–VO interaction ports ($f_i(k), \hat{v}_i(k)$) is bounded. If we attain this N -port passivity (13), by using some available (hybrid) passive device–VO coupling techniques (e.g., virtual coupling [7], [8] or PSPM [9]; see Section III-C) to connect each VO local copy with a (continuous-time passive) haptic device, we would be able to enforce *continuous-time* N -port passivity of the P2P architecture (as experienced by the N users), with the interaction stability, portability, and scalability stated in Section I following as well.

The following proposition shows that, similar to the continuous-time case [34], [35], with the passivity of each local VO simulation (9), we can reduce the problem of enforcing the N -port closed-loop passivity of the P2P architecture (13) into that of the N -port consensus controller passivity: $\forall \bar{M} \geq 0, \exists c \in \mathfrak{R}, \text{ s.t.}$

$$\sum_{k=0}^{\bar{M}} \sum_{i=1}^N \hat{v}_i(k)^T \tau_i(k) T_i^k \leq c^2 \quad (14)$$

i.e., maximum generatable energy from the N consensus control ports ($\tau_i(k), \hat{v}_i(k)$) is bounded. It is usually simpler to prove this controller passivity (14) than the closed-loop passivity (13), since the former involves only (linear) $\tau_i(k)$ and not the VO dynamics (9). In Section III-B, we will design the consensus control $\tau_i(k)$ to satisfy this N -port controller passivity (14), even if the Internet is unreliable with varying delay, packet loss, data swapping, etc., and their topology $\mathcal{G}(\mathcal{V}, \mathcal{E})$ is only partially connected.

Proposition 2: Suppose each VO local copy is discrete-time passive in the sense of (12). Then, discrete-time consensus controller passivity (14) implies discrete-time N -port closed-loop passivity of the P2P architecture (13).

Proof: Substituting (14) into (12), we can obtain (13) with $d^2 := \sum_{i=1}^N d_i^2 + c^2$. ■

²This is still true, even with the consensus control $\tau_i(k)$ in Section III-B and the virtual coupling $f_i(k)$ in Section III-C.

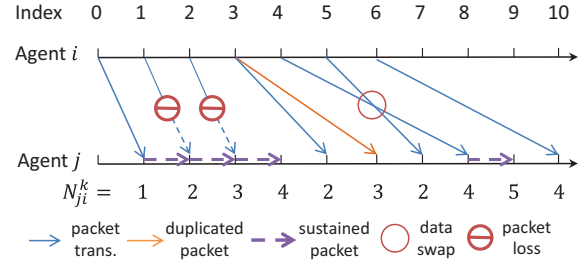


Fig. 4. Indexing delay N_{ji}^k can capture various communication defects.

B. Passive Virtual Object Consensus Over the Internet

Following [2], [3], and [35], we design the consensus control $\tau_i(k)$ in (9) to be composed of PD-type coupling (distributed over the communication graph $\mathcal{G}(\mathcal{V}, \mathcal{E})$) and local damping injection s.t.

$$\begin{aligned} \tau_i(k) := & -B_i \hat{v}_i(k) - \underbrace{\sum_{j \in \mathcal{N}_i} D_{ij} [\hat{v}_i(k) - \delta_{ij}^k \hat{v}_j(k - N_{ij}^k)]}_{\text{D-coupling}} \\ & - \underbrace{\sum_{j \in \mathcal{N}_i} P_{ij} [\hat{x}_i(k) - \hat{x}_j(k - N_{ij}^k)]}_{\text{P-coupling}} \quad (15) \end{aligned}$$

where \mathcal{N}_i is the information neighbors of the i th user; $B_i, P_{ij}, D_{ij} \in \mathfrak{R}^{n \times n}$ are, respectively, the symmetric/positive-definite local damping, P- and D-coupling gain matrices, with P_{ij}, D_{ij} defined on the edge e_{ij} over $\mathcal{G}(\mathcal{V}, \mathcal{E})$ ³; and $N_{ij}^k \geq 0$ is the time-varying (integer) indexing delay (to be defined below) from the j th user to the i th user at the discrete-time index k . We also assume

$$P_{ij} = P_{ji}, D_{ij} = D_{ji} \quad (16)$$

i.e., symmetric P- and D-couplings on the edge e_{ij} , although we allow $N_{ij}^k \neq N_{ji}^k$ (e.g., asymmetric delays) and $P_{ij} \neq P_{pq}, D_{ij} \neq D_{pq}$ for $(i, j) \neq (p, q)$ (i.e., nonuniform P–D couplings).

The indexing delay $N_{ij}^k \geq 0$ is defined as follows: 1) If the packet of a signal \star_j from the j th user is received by the i th user, N_{ij}^k is the k -index difference between i th-site's reception and j th-site's transmission; and 2) if no packet from the j th user is received at k , we set $N_{ij}^k \leftarrow N_{ij}^{k-1} + 1$ with the previous packet being hold (i.e., packet sustainment) (see Fig. 4). This index delay N_{ij}^k can then capture various communication unreliability of the Internet, including varying delay (e.g., master $k = 3, 6$ in Fig. 4), packet loss (e.g., master $k = 1, 2$ in Fig. 4), data swapping (e.g., master $k = 4, 5$ in Fig. 4), and packet duplication (e.g., master $k = 3$ in Fig. 4). We also assume that with the packet sustainment included, $\exists \bar{N}_{ij} \geq 0$ s.t. $N_{ij}^k \leq \bar{N}_{ij} \forall k \geq 0$ (e.g., no complete communication blackout); and $\exists T_j^{\max}, T_j^{\min} > 0$ s.t. $T_j^{\min} \leq T_j^k \leq T_j^{\max}, \forall k \geq 0, j = 1, 2, \dots, N$ (e.g., no crash of local VO simulation).

For the P-action in (15), it is often desirable to sustain the previous set-position data \hat{x}_j , when packets are missing. As

³The results here can be easily extended to asymmetric B_i or positive semidefinite D_{ij} . The VO damping $(1/N)B$ in (9) may also serve the role of local damping [i.e., $B_i := (1/N)B$ for (18)]: We use B_i here to “modularize” the consensus control (15) from the VO simulation (9).

shown later in Theorem 1 and its proof in the Appendix, this set-position holding does not jeopardize N -port passivity of the consensus control (14). Doing so for the set-velocity signal \hat{v}_j in (15), yet, can compromise passivity (14). To prevent this, we insert duplication avoidance function δ_{ij}^k in (15) defined s.t.

$$\delta_{ij}^k := \begin{cases} 0, & \text{if } \hat{v}_j(k - N_{ij}^k) \text{ is duplicated} \\ 1, & \text{otherwise} \end{cases} \quad (17)$$

where the condition of the first line includes both ‘‘real’’ duplication (i.e., due to communication itself) as well as ‘‘artificial’’ duplication (i.e., from packet sustainment). This δ_{ij}^k can be easily implemented by using some packet numbering mechanisms.

We now present the main result of this paper in the following theorem, which shows that, under a certain gain setting condition, even if the Internet communication is unreliable and its topology $\mathcal{G}(\mathcal{V}, \mathcal{E})$ only partially connected, our P2P architecture can guarantee the N -port closed-loop passivity (13), configuration consensus among the N VO local copies when released from the users, and force balance among the users as if they are physically manipulating the VO together.

Theorem 1: Consider the N VO local copies (9) under the consensus control (15) over unreliable Internet communication network with undirected and connected topology $\mathcal{G}(\mathcal{V}, \mathcal{E})$. Suppose we set the gains B_i, P_{ij}, D_{ij} , s.t.

$$B_i \succeq \sum_{j \in \mathcal{N}_i} \left(\frac{\bar{N}_{ij} + \bar{N}_{ji}}{2} T_j^{\max} P_{ij} + \frac{1}{2} \left[\frac{T_j^{\max}}{T_j^{\min}} - 1 \right] D_{ij} \right) \quad (18)$$

for $i = 1, 2, \dots, N$, where $T_j^{\max} := \max_k(T_j^k)$, $T_j^{\min} := \min_k(T_j^k) > 0$, $v_i(k) = 0, \forall k \leq 0$, and $A \succeq B$ (or $A \succ B$, resp.) implies $A - B$ is positive semidefinite (or definite, resp.) for square matrices A, B . Then

- 1) the P2P architecture possesses the discrete-time N -port closed-loop passivity (13);
- 2) if B_i is augmented by an extra positive-definite damping $B_i^e \in \mathbb{R}^{3 \times 3}$ ($B_i^e \succ 0$) and $f_i(k) = 0$

$$\left[\mathcal{P} + I_N \otimes \frac{K}{N} \right] (x(k) - 1_N \otimes x_d) \rightarrow 0 \quad (19)$$

where $x(k) = [x_1(k); x_2(k), \dots, x_N(k)] \in \mathbb{R}^{3nN}$, and $\mathcal{P} \in \mathbb{R}^{3nN \times 3nN}$ is the stiffness matrix (6);

- 3) if $v_i(k) \rightarrow 0$, for all the users

$$\sum_{i=1}^N f_i(k) \rightarrow K(\bar{x}(k) - x_d) \quad (20)$$

where $\bar{x}(k) := (x_1(k) + x_2(k) + \dots + x_N(k))/N \in \mathbb{R}^{3n}$.

Proof: As shown in (38) in the Appendix, under condition (18), the consensus control $\tau_i(k)$ satisfies N -port controller passivity (14) with $c^2 = \sum_{l=1}^{N_e} \varphi_{pq}(0)|_{(p,q) \approx l}$, where $\varphi_{pq}(k) := \|\Delta x_{pq}^k\|_{P_{pq}}^2/4$ with $\Delta x_{pq}^k := x_p(k) - x_q(k)$, i.e., half of the energy stored in P_{pq} on the edge e_{pq} . The discrete-time N -port closed-loop passivity (13) then follows from Proposition 2 with $d^2 := \sum_{i=1}^{N_e} E_i(0) + \sum_{l=1}^{N_e} \varphi_{pq}(0)$, $(p, q) \approx l$.

For the second item, note that, with the extra B_i^e (i.e., $B_i + B_i^e$ instead of B_i for (15) with B_i satisfying (18)), we have, instead of (38), $\sum_{k=0}^{\bar{M}} s_E(k) \leq \sum_{l=1}^{N_e} \varphi_{pq}(0) -$

$\sum_{k=0}^{\bar{M}} \sum_{i=1}^N \|\hat{v}_i(k)\|_{B_i^e}^2 T_i^k$. Combining this with (12), we can then show that $\forall \bar{M} \geq 0$

$$\sum_{i=1}^N \sum_{k=0}^{\bar{M}} \hat{v}_i(k)^T f_i(k) T_i^k \geq -d^2 + \sum_{k=0}^{\bar{M}} \sum_{i=1}^N \|\hat{v}_i(k)\|_{B_i^e}^2 T_i^k$$

i.e., the system is still N -port closed-loop passive (13), with the extra dissipation due to B_i^e . If $f_i(k) = 0$, we then have

$$d^2 \geq \sum_{k=0}^{\bar{M}} \sum_{i=1}^N \|\hat{v}_i(k)\|_{B_i^e}^2 T_i^k, \forall \bar{M} > 0$$

implying that, with d bounded and $T_i^k > 0$, $\hat{v}_i(k) \rightarrow 0$.

From (9) with $\hat{v}_i(k) \rightarrow 0$, we have $x_i(k+1) \rightarrow x_i(k)$ and $\hat{x}_i(k+1) \rightarrow \hat{x}_i(k)$. This then implies that $K(\hat{x}_i(k+1) - x_d) \rightarrow K(\hat{x}_i(k) - x_d)$ for (9) as well as $\tau_i(k+1) \rightarrow \tau_i(k)$ for (15), with $\hat{x}_j(k+1) \rightarrow \hat{x}_j(k) \rightarrow \dots \rightarrow \hat{x}_j(k+1 - N_{ij}^k) \rightarrow \hat{x}_j(k - N_{ij}^k)$. Applying this observation to (9) for T_i^k and T_i^{k+1} integration steps, we can achieve

$$\frac{v_i(k+1) - v_i(k)}{T_i^k} \rightarrow \frac{v_i(k+2) - v_i(k+1)}{T_i^{k+1}}$$

where $v_i(k+2) \rightarrow v_i(k)$ from $\hat{v}_i(k+1) \rightarrow \hat{v}_i(k) \rightarrow 0$. Thus, we have $(1/T_i^k + 1/T_i^{k+1})(v_i(k+1) - v_i(k)) \rightarrow 0$, i.e., $v_i(k+1) \rightarrow v_i(k)$, which, with $\hat{v}_i(k) \rightarrow 0$, further implies $v_i(k) \rightarrow 0$. Reflecting this back into (9) with $f_i(k) = 0$, we can then achieve

$$\frac{K}{N}(x_i(k) - x_d) + \sum_{j \in \mathcal{N}_i} P_{ij}(x_i(k) - x_d - x_j(k) + x_d) \rightarrow 0$$

$\forall i \in \{1, 2, \dots, N\}$, which can be written as (19).

For the third item, similar to the aforementioned derivation, using $v_i(k) \rightarrow 0$ for (9), we have $\hat{x}_i(k) \rightarrow x_i(k)$ and

$$\frac{K}{N}(x_i(k) - x_d) + \sum_{j \in \mathcal{N}_i} P_{ij}(x_i(k) - x_j(k)) \rightarrow f_i(k).$$

Summing this up, we can have

$$\sum_{i=1}^N f_i(k) \rightarrow K(\bar{x}(k) - x_d) + \sum_{i=1}^N \sum_{j \in \mathcal{N}_i} P_{ij}(x_i(k) - x_j(k))$$

where the most right term is zero, since, from $\mathcal{G}(\mathcal{V}, \mathcal{E})$ being undirected and $P_{ij} = P_{ji}$, for each $P_{ij}(x_i(k) - x_j(k))$, we also have $P_{ji}(x_j(k) - x_i(k))$, with their sum being zero. ■

Here, the discrete-time index k need not be (absolute-time) synchronized among the users, and each user need not precisely track their own or neighbors' k to implement (15). In fact, to implement (15), each i th user can simply receive/collect the data from the neighbors (i.e., $(\hat{x}_j(k - N_{ij}^k), \hat{v}_j(k - N_{ij}^k))$), check the duplication (17), apply the consensus control (15) to their local VO simulation (9), solve for $(\hat{x}_i(k), \hat{v}_i(k))$, and send them to their neighbors over the Internet. All of these processes do not require each i th user knowing N_{ij}^k and T_j^k either. The passivity condition (18) can also be enforced *locally* by using that $\bar{N}_{ij} + \bar{N}_{ji} \leq \bar{N}_{iji} + \bar{N}_{jij}$ (from $\bar{N}_{ji} \leq \bar{N}_{iji}$) along with the information of T_j^{\max}, T_j^{\min} , where \bar{N}_{iji} is the maximum round-trip delay, which each i th user can measure by locally counting their own index k between sending a packet to and

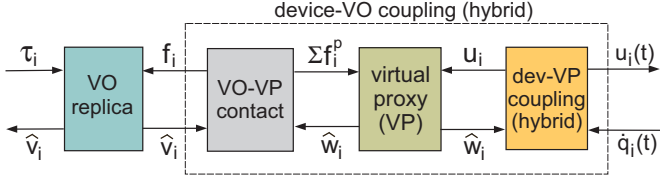


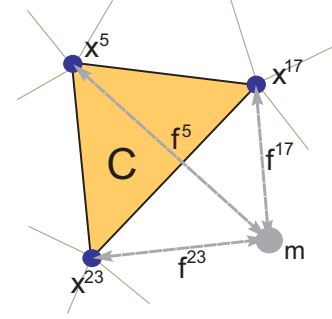
Fig. 5. Network representation of device-VO coupling.

receiving its acknowledgment from the j th user. In this paper, we also assume that the (fictitious) instance of $k = 0$ of all users starts similarly in absolute time, and T_i^k is more or less uniform across users and much faster than the communication rate to prevent excessively large N_{ij}^k (e.g., $N_{ij}^k \rightarrow +\infty$ if $T_j^k \gg T_i^k$) or negative $N_{ij}^k < 0$.

The consensus property (19) implies that, when released, $x(k) = [x_1(k); x_2(k); \dots; x_N(k)] \in \mathbb{R}^{3nN}$ will converge to the set $\ker(\mathcal{P}) \cap \ker(I_N \otimes K)$, where the former captures the consensus P-action P_{ij} over the connected $\mathcal{G}(\mathcal{V}, \mathcal{E})$, while the latter captures the VO spring connection K in (10): 1) if $K = 0$ for (9), following Proposition 1, $\tau_i(k)$ in (15) will push $x_i(k) \rightarrow x_j(k) \rightarrow a$ with an unspecified $a \in \mathbb{R}^{3n}$, implying that all VO local copies will consensus to the same yet arbitrary shape a ; 2) if $K = K_{\text{int}}$ with an undirected and connected $\mathcal{G}_{VO}(\mathcal{X}, \mathcal{K})$ and $K_{\text{gnd}} = 0$, we will have $x_i(k) \rightarrow x_j(k) \rightarrow x_d + I_n \otimes z$ with an unspecified $z \in \mathbb{R}^3$ (cf., Section III-A), i.e., all the VO local copies will attain the same (undeformed) shape x_d , yet, possibly “floating” by the same but arbitrary $E(3)$ -displacement z (i.e., symmetry in $E(3)$ [32]); and 3) if $K_{\text{gnd}} \neq 0$ with the aforementioned K_{int} , K will become positive definite, $x_i(k) \rightarrow x_d$, and all the VO copies will converge to the same shape at the same $E(3)$ -location (i.e., breaking symmetry in $E(3)$ [32]).

On the other hand, the force balance property (20) shows that our P2P architecture indeed captures the peculiarity of multiuser shared haptic interaction, i.e., 1) possibly geographically distributed N users can now interact with each other via the shared deformable VO, as if they are physically manipulating it together, while inducing the collective deformation $\bar{x}(k)$ on it; and 2) if only the i th user alone pushes the object with perfect consensus among the N VO local copies (i.e., $x_i(k) = x_j(k)$); from (20), we have $f_i(k) \rightarrow K(x_i(k) - x_d)$, implying that this user i will perceive the “intended” VO with its stiffness being K [not K/N as in (9)] just like in the case of single-user haptics with the unscaled VO (9) (i.e., $N = 1$). Note also from (15) that, with an adequate consensus performance (i.e., $x_i(k) \approx x_j(k)$; e.g., best topology in Section V), we will have $\|\tau_i(k)\| \approx 0$, implying that the effect of the consensus control (15) on each user’s perception of the shared VO would not be significant. See the last statement of Section III-C as well.

Although the results of Theorem 1 are for the discrete-time domain, we would be able to transfer them to the continuous-time domain (i.e., as experienced by the real N users), if we use some suitable passive *hybrid* device-VO coupling for the P2P architecture in Fig. 2 and extend Theorem 1 to the continuous-time domain (e.g., virtual coupling [7], [8]; PSPM [9]). Even if it is rather a generic problem in haptics and not the main concern of this paper, for completeness and expedited implementation of our P2P architecture, in Section III-C, we briefly discuss this


 Fig. 6. Contact mesh \mathcal{C} , contact node x^* , contact force f^* , and VP m .

issue of passive device-VO coupling, particularly how to utilize the well-known virtual coupling technique [7], [8] for that.

C. Passive Device-VO Coupling

At the local site of each user, we implement *hybrid* device-VO coupling, as shown in Fig. 5, where the virtual proxy (VP), which is connected to the device through the device-VP coupling, interacts with the VO local copy via the VO-VP contact block. To enforce (discrete-time) passivity of this VP, similar to (9), we utilize the NPMI algorithm [5]: For the i th user

$$\begin{aligned} m_i \frac{w_i(k+1) - w_i(k)}{T_i^k} &= u_i(k) + \sum_{p \in \mathcal{C}_i} f_i^p(k) \\ \hat{w}_i(k) &:= \frac{w_i(k+1) + w_i(k)}{2} = \frac{y_i(k+1) - y_i(k)}{T_i^k} \\ \hat{y}_i(k) &:= \frac{y_i(k+1) + y_i(k)}{2} \end{aligned} \quad (21)$$

where $m_i > 0$, $y_i(k), w_i(k) \in \mathbb{R}^3$ are, respectively, the mass, position, and velocity of VP; T_i^k is the integration step in (9); and $f_i^p(k), u_i(k) \in \mathbb{R}^3$ are the VO-VP contact force and the device-VP coupling force, both to be explained in the following.

We define the VO-VP contact force $f_i^p(k) \in \mathbb{R}^3$ in (21) by

$$f_i^p(k) := \begin{cases} -b_c[\hat{w}_i(k) - \hat{v}_i^p(k)], & \text{if } p \in \mathcal{C}_i^k \\ -k_c[\hat{y}_i(k) - \hat{x}_i^p(k)] & \\ 0, & \text{otherwise} \end{cases} \quad (22)$$

where $\mathcal{C}_i^k \in \mathcal{X}$ denotes the “contact mesh” consisting of “contact nodes” of the VO of the i th user at k (see Fig. 6). Among the VO’s nodes, only these contact nodes interact with the VP. This implies that 1) for $f_i(k) = [f_i^1(k); f_i^2(k); \dots; f_i^n(k)] \in \mathbb{R}^{3n}$ in (9), $f_i^j(k) = 0$ if $j \notin \mathcal{C}_i^k$, and 2) the total VP-VO contact force in (21) is given by

$$\sum_{p \in \mathcal{C}_i^k} f_i^p(k) = -[1_n^T \otimes I_{3 \times 3}] f_i(k) \quad (23)$$

where $1_n = [1; 1; \dots; 1] \in \mathbb{R}^n$, and \otimes is the Kronecker product.

How to passively detect and render this VO-VP contact, particularly when the contact switches on and off, is still an open problem in haptics. We do not attempt to solve it here, and rather simply assume that this VO-VP contact block is discrete-time

two-port passive: $\forall \bar{M} \geq 0, \exists c_{ci} \in \mathfrak{R}, \text{ s.t.}$

$$\sum_{k=0}^{\bar{M}} [\hat{v}_i^T(k) f_i(k) + \sum_{p \in \mathcal{C}_i^k} \hat{w}_i^T(k) f_i^p(k)] T_i^k \leq c_{ci}^2 \quad (24)$$

for all $i \in \{1, 2, \dots, N\}$, which is more or less reasonable when the update rate T_i^k is fast enough as for our experiment in Section V (with $T_i^k = 2$ ms). This VO–VP contact passivity is always granted if the contact is maintained with the same contact nodes all the time, which can be easily shown by using (9) and (21) to obtain (24) with $c_{hi}^2 := \sum_{p \in \mathcal{C}_i} \|x_i^p(0) - y_i(0)\|^2/2$. See also [5] for passive VO–VP contact handling when the VO is a 1-D virtual wall.

On the other hand, for the device–VP coupling $u_i(k)$ in (21), we briefly explain here how to utilize the well-known virtual coupling technique⁴ [6]–[8]. For this, define the device–VP coupling as follows: During T_i^k and for $t \in T_i^k \approx [t_i^k, t_i^{k+1})$ with t_i^k denoting the absolute-time instance of the onset of T_i^k

$$\begin{aligned} u_i(k) &:= -b_v^i \hat{w}_i(k) \\ &\quad - B_{vc}^i (\hat{w}_i(k) - \hat{v}_{k-1}^i) - K_{vc}^i (\hat{y}_i(k) - q_i^k) \\ u_i(t) &:= -b_d^i \dot{q}_i(t) \\ &\quad - B_{vc}^i (\hat{v}_{k-1}^i - \hat{w}_i(k-1)) - K_{vc}^i (q_i^k - y_i(k)) \end{aligned}$$

where $q_i(t) \in \mathfrak{R}^3$ is the haptic device configuration, with q_i^k being its sampling at t_i^k ; $u_i(t) \in \mathfrak{R}^3$ is the device control torque; $\hat{v}_{k-1}^i := (q_i^k - q_i^{k-1})/T_i^{k-1}$; $b_v^i, b_d^i > 0$ is the (extra) VP damping and the (minimum) device damping; and $B_{vc}^i, K_{vc}^i > 0$ are the virtual coupling gains. Here, $u_i(t)$ is computed at t_i^k and applied through t_i^{k+1} , while $u_i(k)$ is used along with $f_i^p(k)$ (and $f_i(k)$) in (22) and $\tau_i(k)$ in (15) to solve the VO-dynamics (9) and the VP-dynamics (21) together over T_i^k , which can still be cast into the noniterative form of (11) with $z_i(k) := [v_i(k); x_i(k); w_i(k); y_i(k)] \in \mathfrak{R}^{6(n+1)}$.

Following [6, Th. 2], we can then show that this virtual coupling $(u_i(k), u_i(t))$ is passive, i.e., $\forall \bar{M} \geq 0, \exists c_{hi} \in \mathfrak{R} \text{ s.t.}$

$$\int_0^{\bar{t}_i} u_i^T(t) \dot{q}_i(t) dt + \sum_{k=0}^{\bar{M}} \hat{w}_i^T(k) u_i(k) T_i^k \leq c_{hi}^2 \quad (25)$$

with $\bar{t}_i := t_i^{\bar{M}+1}$, if the following conditions are met:

$$\begin{aligned} b_d^i &\geq B_{vc}^i \left(\frac{T_i^k}{T_i^{k-1}} + 1 \right) + K_{vc}^i T_i^k \\ b_v^i &\geq \frac{B_{vc}^i}{2} \left(\frac{T_i^k}{T_i^{k-1}} - 1 \right) + \frac{K_{vc}^i T_i^k}{2}. \end{aligned} \quad (26)$$

For a complete proof, see [6]. Combining (24) and (25) with the VP's open-loop passivity, i.e., similar to (12), from (21)

$$\sum_{k=0}^{\bar{M}} \hat{w}_i^T(k) [u_i(k) + \sum_{p \in \mathcal{C}_i^k} f_i^p(k)] T_i^k \geq -\kappa_i(0)$$

⁴For the device–VP coupling, PSPM [9] may also be used with its passivity condition less conservative than (26). See [9] for more details.

$\forall \bar{M} \geq 0$, where $\kappa_i(k) := \|w_i(k)\|_{m_i}^2/2$, we can also achieve hybrid two-port passivity of the total device–VO coupling in Fig. 5 s.t.

$$\int_0^{\bar{t}_i} u_i^T(t) \dot{q}_i(t) dt + \sum_{k=0}^{\bar{M}} \hat{v}_i^T(k) f_i(k) T_i^k \leq \kappa_i(0) + c_{ci}^2 + c_{hi}^2$$

for all $\bar{M} \geq 0, i = 1, 2, \dots, N$.

With each user's device also being continuous-time passive, this (hybrid) passivity of the device–VO coupling then bridges the discrete-time N -port passivity of the P2P architecture (item 1 of Theorem 1) to its continuous-time N -port passivity (as experienced by the users via their haptic devices). With this passive energetics and the PD-structure of the device–VO coupling, we would also be able to duplicate Theorem 1 for the continuous-time domain, the detail of which we omit here and refer to [3] and [9], since it would involve technical derivations/arguments similar to those therein (i.e., with enough damping, $(\dot{q}_i(t), v_i(k), w_i(k)) \rightarrow 0$; position/force coordination follows from Barbalat's lemma like argument for the hybrid closed-loop system with spring connections).

Note that the passivity conditions of our P2P architecture, (18) and (26), impose no restrictions whatsoever on the structural parameters of VO and VP simulations [i.e., M, B, K , and m_i in (9) and (21)]. This then implies that 1) VO dynamics can be designed regardless of the physical construction/parameters of the devices to be engaged and the state of the Internet communication during operation (simulation-device/communication separation); 2) VP's mass m_i can be set very small (sharper force feedback); and 3) any users can join the P2P architecture, while keeping the same VO and consensus coupling even if their devices' damping is small (portability). These (powerful) properties, endowed by the passivity of NPMI-based VO and VP simulations (9) and (21), are in a stark contrast with the current practice in haptics, where VO/VP parameters are typically bound to the device damping (e.g., minimum mass [13]). In addition, suppose that N_{ij}^k is very small and T_j^k is almost constant. We can then employ very large D_{ij}, P_{ij} (i.e., rigid consensus coupling) while satisfying (18); thus, if each user's device–VO coupling (see Fig. 5) can also be made rigid enough, (near) ideal multiuser shared haptic interaction will be achieved (i.e., each user perceives almost exactly as if physically collaborating on a real deformable object, whose dynamics is given by (9) with $N = 1$).

IV. NETWORK TOPOLOGY OPTIMIZATION

Performance of our P2P architecture strongly depends on how fast the convergence of the consensus control is, or equivalently, how fast information propagates among the users over the Internet via the consensus control. This information propagation would likely be fastest if all the users communicate with all the others. Such all-to-all communication (i.e., fully connected $\mathcal{G}(\mathcal{V}, \mathcal{E})$), yet, is often infeasible or prohibitively expensive particularly when the number of users (N) and/or the dimension of VO ($3n$) are large (e.g., bandwidth limitation). It is rather more reasonable, under the current Internet technology, to assume that only few communication links are possible for each user or only a limited number of links are available for the whole P2P architecture.

Then, the question would be which graph we should choose from the set of such practically feasible network topologies $\mathcal{G}_F := \{\mathcal{G}(\mathcal{V}, \mathcal{E}_1), \mathcal{G}(\mathcal{V}, \mathcal{E}_2), \dots, \mathcal{G}(\mathcal{V}, \mathcal{E}_m)\}$ to maximize the speed of information propagation (i.e., fastest mixing graph [36]). For this, we assume that a simple first-order consensus model can adequately capture the information propagation among the users through the consensus control, with P_{ij} defining the information mixing strength and the (constant) average of $N_{ij}^k T_i^k$ specifying the information propagation delay for each link e_{ij} . As shown by the experimental results in Section V, this simplifying assumption appears to be reasonable.

More precisely, we use the following widely used first-order consensus equation to model the information propagation among the N users:

$$p_i(k+1) = \left(\sum_{j \in \mathcal{N}_i} P_{ij} \right)^{-1} \sum_{j \in \mathcal{N}_i} P_{ij} p_j(k+1 - N_{ij})$$

where $p_i(k) \in \mathbb{R}^n$ defines an abstract state of information of the i th user at the time index k , and N_{ij} represents the averaged delaying effect of $N_{ij}^k T_i^k$ defined by

$$N_{ij} := \mathcal{Z} \left[\frac{\sum_{k=1}^{\bar{M}} N_{ij}^k T_i^k / \bar{M}}{\sum_{i=1}^N \sum_{k=1}^{\bar{M}} T_i^k / (\bar{M}N)} \right]$$

where $\mathcal{Z}[\star]$ is an integer closest to $\star \in \mathbb{R}$ with $\bar{M} > 0$ a large enough averaging interval.

This first-order information mixing model can then be ‘‘lifted’’ into the following form:

$$\begin{bmatrix} p(k+1) \\ p(k) \\ \vdots \\ p(k+1 - \bar{N}) \end{bmatrix} = J(\mathcal{G}, P_{ij}, N_{ij}) \begin{bmatrix} p(k) \\ p(k-1) \\ \vdots \\ p(k - \bar{N}) \end{bmatrix}$$

where $p(k) := [p_1(k); p_2(k) \dots; p_N(k)] \in \mathbb{R}^{nN}$; $\bar{N} = \max_{ij} (N_{ij})$

$$J(\mathcal{G}, P_{ij}, N_{ij}) := \begin{bmatrix} A_0 & A_1 & \dots & A_{\bar{N}-1} & A_{\bar{N}} \\ I & 0 & \dots & 0 & 0 \\ 0 & I & \ddots & 0 & \vdots \\ \vdots & 0 & \ddots & \ddots & \vdots \\ 0 & \dots & 0 & I & 0 \end{bmatrix}$$

and $A_k \in \mathbb{R}^{nN \times nN}$ has its $n \times n$ ij th component given by

$$A_k^{ij} = \begin{cases} \left(\sum_{j \in \mathcal{N}_i} P_{ij} \right)^{-1} P_{ij}, & \text{if } k = N_{ij} \text{ and } e_{ij} \in \mathcal{E} \\ 0_{n \times n}, & \text{otherwise.} \end{cases}$$

The matrix $J(\mathcal{G}, P_{ij}, N_{ij}) \in \mathbb{R}^{nN(\bar{N}+1) \times nN(\bar{N}+1)}$ then defines the information propagation among the users. We also found that, with connected $\mathcal{G}(\mathcal{V}, \mathcal{E})$, $J(\mathcal{G}, P_{ij}, N_{ij})$ has n -eigenvalues at 1 with eigenvectors $\mathbf{1}_{\bar{N}+1} \otimes \mathbf{1}_N \otimes a$ with arbitrary $a \in \mathbb{R}^n$, and all the other eigenvalues strictly within the unit circle. That is, the n -eigenvalues at 1 correspond to the (steady-state) information consensus state (i.e., $p_i(k) \rightarrow p_j(k) \rightarrow a$), while the remaining $nN(\bar{N}+1) - n$ eigenvalues are related to

the (transient) nonconsensus residual, which is vanishing, since the spectral radius of all these eigenvalues is < 1 . This then suggests the optimal network topology from \mathcal{G}_F to be the one with the minimum $(n+1)$ th largest spectral radius λ_{n+1} , i.e., the solution of the following optimization problem:

$$\min_{\mathcal{G} \in \mathcal{G}_F} |\lambda_{n+1}(J(\mathcal{G}, P_{ij}, N_{ij}))|. \quad (27)$$

If $P_{ij} = p_{ij} I_n$ with a scalar $p_{ij} > 0$, (27) can be further simplified with scalar information state $p_i(k) \in \mathbb{R}$, reduced dimension of $J(\mathcal{G}, P_{ij}, N_{ij}) \in \mathbb{R}^{N(\bar{N}+1)}$ with only one eigenvalue at 1 and all the others strictly within the unit circle, and λ_{n+1} replaced by λ_2 (algebraic connectivity [37]). Although there are numerous results on (similar) network optimization problems (e.g., [38]–[40]), here, we adopt more ‘‘consensus-based’’ approach (27) similar to [36] and [37], since by doing so, we could directly migrate our consensus control (15) into the optimization problem (27), while also explicitly incorporating nonuniform mixing intensities P_{ij} among the users as well. A thorough comparison of our ‘‘consensus-based’’ approach (27) (as well as [36] and [37]) with other well-known network optimization techniques (e.g., [38]–[40]) is beyond the scope of this paper and a topic for future research.

V. EXPERIMENTS

We use our P2P control architecture to implement a four-user haptic interaction system over the Internet. Three Phantom Omnis and one Phantom Desktop from Sensable are deployed as the haptic devices (each with three Cartesian actuated degrees of freedom). A ball-like deformable VO, which is shown in Fig. 3, is chosen as the shared VO, with $M = 0.04 I_{3n}$ kg, $B = 0$ N·s/m, and $K_{\text{int}}^{rs} = 100 I_3$ N/m, which connects VO’s 33 nodes over the structure graph $\mathcal{G}_{VO}(\mathcal{X}, \mathcal{K})$ via surface and internal meshes. No mechanical ground is assumed (i.e., $K_{\text{gnd}} = 0$) so that the VO can float in $E(3)$. We also set the following parameters to be the same for all users: integration step $T_i^k =: T = 2$ ms (see [6] for single-user haptics with varying T_i^k); VP mass $m_i = 0.001$ kg; contact gains $b_c = 0$ N·s/m and $k_c = 200$ N/m; and virtual coupling gains $B_{vc} = 0$ N·s/m, $K_{vc} = 200$ N/m, and $b_{vi} = 2$ N·s/m to satisfy (26). Here, we intentionally set B, b_c, B_{vc} all to be zero to show that, even with this lack of damping (i.e., prone to oscillate), our proposed control framework, due to its passivity enforcing with (18) and (26), can still ensure the stability of total P2P architecture over unreliable and partially connected communication network.

We also use a simple stochastic model⁵ to achieve Internet-like communication. For this, we first set the mean delay of each communication link s.t.

$$[N_{ij}T] = \begin{bmatrix} 0 & 4 & 4 & 4 \\ 8 & 0 & 80 & 200 \\ 4 & 100 & 0 & 200 \\ 6 & 240 & 200 & 0 \end{bmatrix} \text{ [ms]}$$

where the ij th element is the average delay on $e_{ij} \in \mathcal{E}$. We allow the actual delay $N_{ij}^k T$ to randomly vary between 50% and 150%

⁵The main goal of this section is to experimentally verify 1) the theoretical results of Theorem 1 (i.e., passivity and steady-state convergence) and 2) the importance/validity of network topology optimization given in Section IV, for which we think our simple stochastic Internet model and $[N_{ij}T]$ values given in the following are adequate, although not necessarily realistic (cf., [41] and [42]).

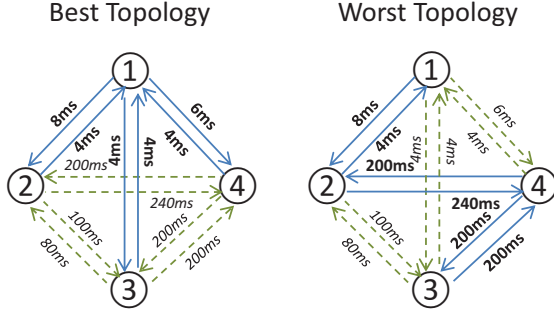


Fig. 7. Best and worst network topologies with average round-trip delays.

of this mean delay $N_{ij}T$ following the uniform distribution. This N_{ij}^k is then applied to each outbound packet $\star_j(k)$, in addition to 5% packet-loss rate and 1% packet-duplication rate, which are uniform across all e_{ij} (once duplicated, a new N_{ij}^k is computed and applied to $\star_j(k)$).

For the consensus control (15), we also choose its gains s.t.

$$P_{ij} = P_{ji} = 1000 \left[\frac{I_{3n}}{2} + \frac{K_{\text{int}}}{2\lambda_{\text{max}}(K_{\text{int}})} \right] [\text{N/m}]$$

$$D_{ij} = D_{ji} = 5I_{3n} [\text{N}\cdot\text{s/m}]$$

for all e_{ij} , where we inject the cross-coupling term $K_{\text{int}}/2\lambda_{\text{max}}(K_{\text{int}})$ to enhance the consensus performance. Given these consensus gains and $[N_{ij}T]$ above, which we found still adequately captures each link's mean delay, we perform the network topology optimization of Section IV with the condition that only three undirected communication links are available for the P2P architecture. The best and worst topologies are shown in Fig. 7. We also found upper bound of each user's $\sum_{j \in \mathcal{N}_i} (\bar{N}_{ij} + \bar{N}_{ji})T/2$ in (18) to be 1) (25, 10, 7, 9)[ms] for the best topology; and 2) (10, 375, 330, 695)[ms] for the worst topology. Then, following (18), we set the local damping B_i in (15) for the four users s.t.: 1) (26.25, 10.5, 7.5, 9.5)[N·s/m] for the best topology; and 2) (10.5, 395, 346.5, 730)[N·s/m] for the worst topology.

Experimental results are presented in Figs. 8 (for the best topology) and 9 (for the worst topology), where 1) top plots show the deformation of four VO local copies (only surface nodes/meshes rendered; deformation drawn three-times exaggerated for presentation purpose) of each user's VP (red) and their contact mesh/nodes (black); 2) middle plots show the x -position of each user's node 19, which is on the second user's contact mesh (i.e., $x^{19} \in \mathcal{C}_2$), as well as the device x -axis control force (u_i^x) of all the users and their sum ($\sum u_i^x$); 3) bottom plots show the positions of device (xd_i, yd_i) and VP (xv_i, yv_i), and the positions of one same node on the denoted user's contact mesh for each user (e.g., $x_1^{15} \in \mathcal{C}_1$ or $y_i^{23} \in \mathcal{C}_3, \forall i = 1, 2, 3, 4$). The four users start by making a light contact with their own VO local copy (first row of top plots of Figs. 8 and 9). Then, they push their own VO copies individually through different contact meshes along different directions (each VP is beneath their contact mesh (black), thus not shown in the second–fourth rows of top plots of Figs. 8 and 9). After the steady state is attained, all

the users release their VO, and four VO copies converge back to the undeformed ball shape.

From Figs. 8 and 9, we can then see that 1) [top plots] even if four (disjoint) VO local copies are individually manipulated, with the consensus control (15), the users can haptically collaborate with each other, while perceiving others' action on the same VO; 2) [middle plots] when released (after 12 s in Fig. 8 and 64 s in Fig. 9), the four VO copies reach their configuration consensus (i.e., item 2 of Theorem 1); 3) [middle plots] multiuser force balance is achieved during (steady-state) collaborative holding of the VO (between 6 and 12 s in Fig. 8 and between 40 and 60 s in Fig. 9) with $\sum_{i=1}^N u_i^x = 0$, which is because $\sum_{i=1}^N \sum_{p \in \mathcal{C}_i} f_i^p = -(1_n^T \otimes I_{3 \times 3}) \sum_{i=1}^n f_i \rightarrow -(1_n^T \otimes I_{3 \times 3}) K(\bar{x} - x_d) = 0$, from (23) and (20) with $(1_n^T \otimes I_{3 \times 3}) K_{\text{int}} = 0$; and 4) [bottom plots] for each user, the device penetrates deeper into VO than VP and VP than the contact nodes, while the (same) contact nodes of other users are pulled by the consensus control, even though each user makes contact on different parts of VO.

Note also that the multiuser haptic interaction in Figs. 8 and 9 is stable, even with the Internet's communication unreliability (e.g., packet loss, varying delay, data swapping, etc). This is due to our enforcing of the N -port passivity (i.e., item 1 of Theorem 1). To verify this claim, we intentionally violate the passivity condition (18) by reducing the local damping B_i to (14, 5, 4, 5) [N·s/m] for the best topology. The result is shown in Fig. 10, where with only a small perturbation exerted by one user on his local VO copy around 2.5 s, the system becomes unstable, clearly manifesting the importance of the N -port passivity (13) and enforcing the condition (18).

The top plots of Figs. 8 and 9 also show a vivid performance difference between the best and worst topologies: To achieve similar deformation of the shared VO (with similar human force), it takes much less time with the best topology (e.g., 3 s for Fig. 8, and 29 s for Fig. 9). The relatively large device–VP deformation in the bottom plots of Figs. 8 and 9 is due to the compliance of the virtual coupling (see Section III-C), implying that, even with the best topology, the VO would feel “softer” than originally designed for in (9). Using (less conservative) passive set-position modulation (PSPM) [9], we may reduce this device–VP deformation (e.g., twice larger K_{vc} possible than for (26) [9, Remark 1], the details of which, yet, we do not provide here and rather refer readers to [9], since this is a standard problem in (single user) haptics and not the main concern of this paper.

As the communication unreliability becomes severer, the performance of our P2P architecture would degrade, being sluggish with a large B_i required for (15) or, equivalently, providing only a dull perception of other users' action on the shared VO with P_{ij}, D_{ij} required to be small for (15). In addition, with such severe delay and loss rate, the consensus control itself (15) would also become sluggish (or slow), possibly affecting (or “masking”) each user's perception of the VO. Such (transient) performance deterioration is typical for many “time-invariant” teleoperation/haptics schemes (e.g., [35], [43]), including our PD-type consensus control (15) and virtual coupling in Section III-C, in which the worst case gains are blindly applied all the time no matter what.

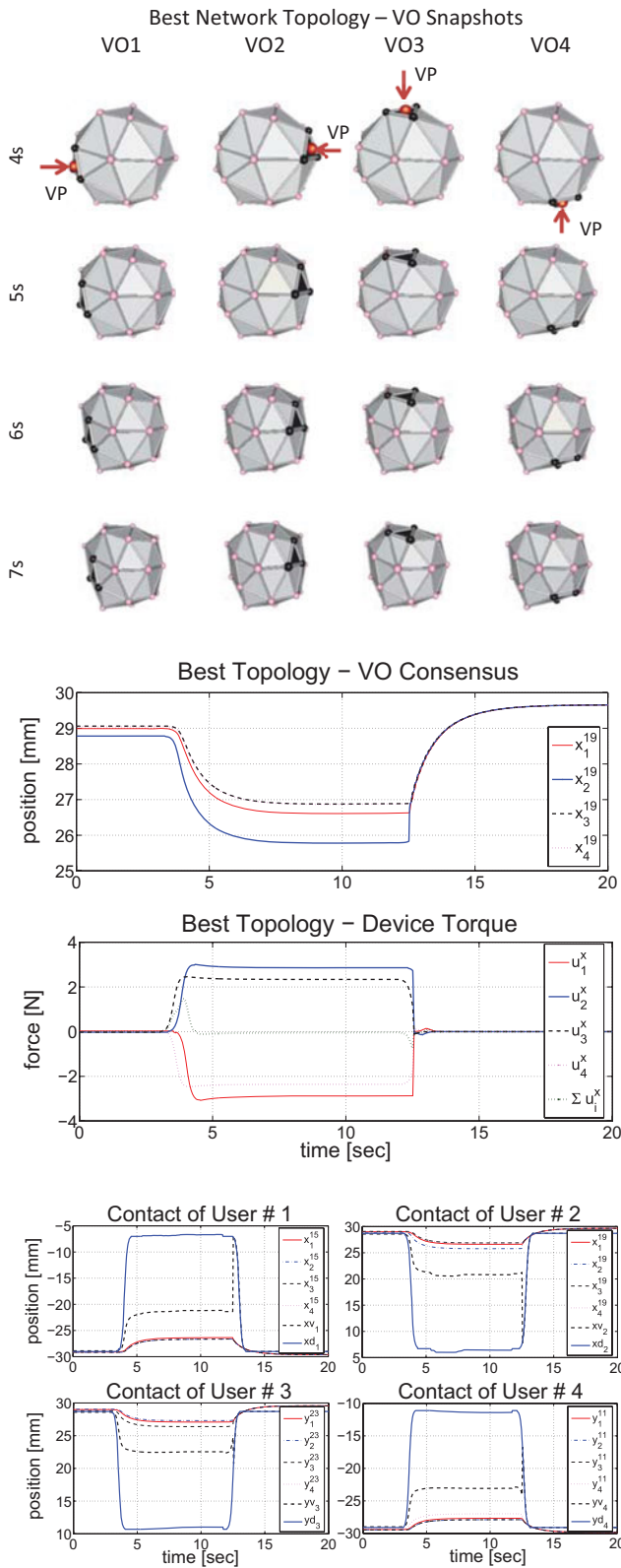


Fig. 8. Experimental results with best topology. (Top) Deformation of VO with contact mesh (black) and VP (red). (Middle) Position a representative node (x_i^{19}) and device control force (u_i^x) of all the users. (Bottom) Positions of device (x_{d_i}, y_{d_i}), VP (x_{v_i}, y_{v_i}), and a node (x_i^r, y_i^r) on the contact mesh of each user.

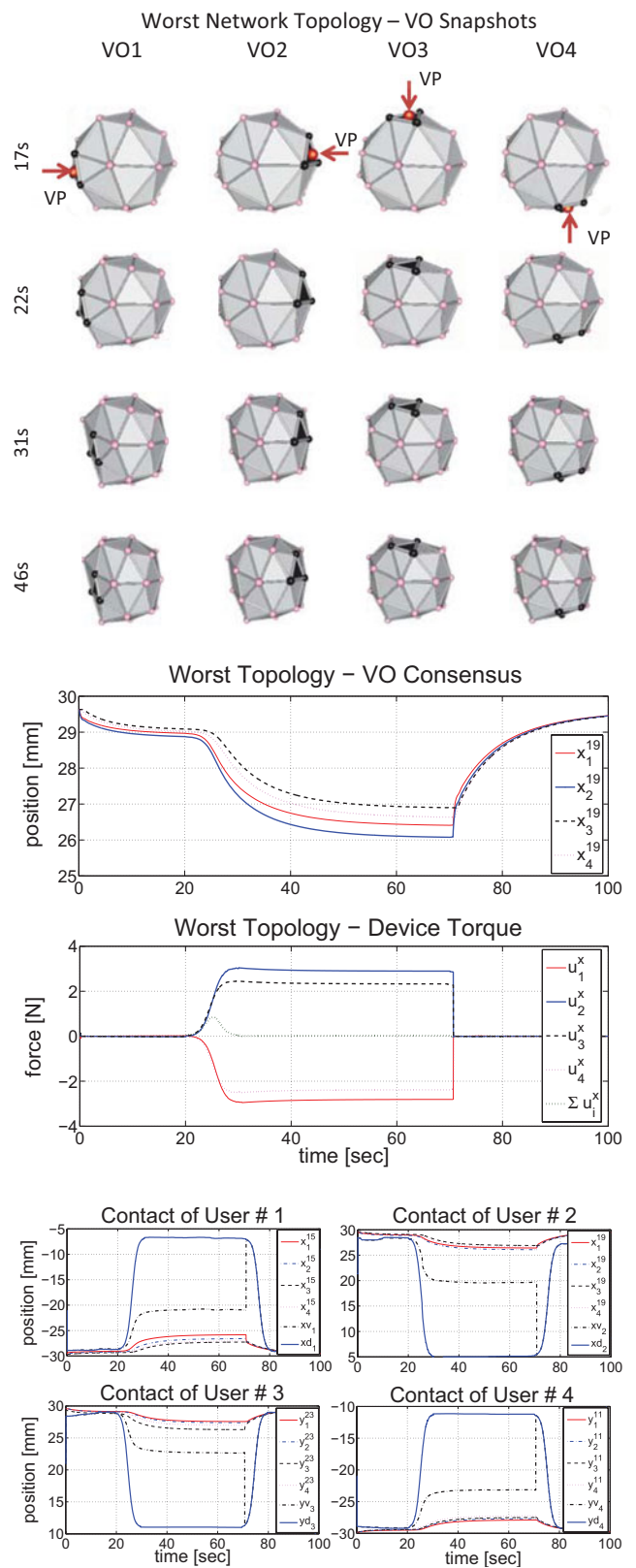


Fig. 9. Experimental results with worst topology. (Top) Deformation of VO with contact mesh (black) and VP (red). (Middle) Position a representative node (x_i^{19}) and device control force (u_i^x) of all the users. (Bottom) Positions of device (x_{d_i}, y_{d_i}), VP (x_{v_i}, y_{v_i}), and a node (x_i^r, y_i^r) on the contact mesh of each user.

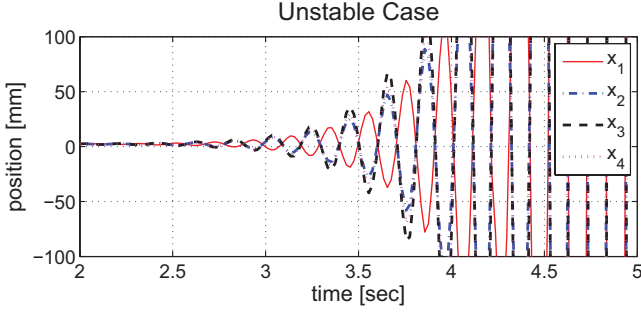


Fig. 10. Unstable behavior with condition (18) intentionally violated: x -axis position of each user's node 9 (i.e., x_i^9) is shown.

How to improve the performance of our PD-type P2P architecture, particularly when the communication is poor, is a topic for future research. For this, we think that our recently proposed PSPM technique [9] is particularly promising, due to its (much) less conservativeness (i.e., higher performance via selective activation of passifying action only when necessary), versatility (e.g., incorporation of estimator/prediction or other consensus algorithms [44]), and flexibility [e.g., estimation of $\bar{N}_{ij} + \bar{N}_{ji}$ in (18) not necessary; completely arbitrary T_i^k possible (cf., statement after Theorem. 1)], on top of, of course, its enforcing of N -port passivity of the P2P architecture.

VI. CONCLUSION

In this paper, a novel P2P control architecture has been proposed for the multiuser shared haptic interaction over the Internet. For haptic feedback responsiveness, each user simulates their own local copy of the shared deformable VO and locally interacts with it, while for haptic experience consistency, these VO local copies are synchronized by the PD-type consensus control over the Internet with undirected, yet only partially connected, communication topology. By extending/utilizing the results of [1]–[3], passivity of the P2P architecture is guaranteed, even if the Internet is imperfect (e.g., with varying delay, packet loss, data swapping, etc), thereby, rendering the architecture interaction stable, portable, and scalable against heterogeneous users/devices. Consensus among the VO local copies and the multiuser force balance via the shared deformable VO are shown. Network topology optimization using algebraic connectivity has also been proposed along with some experimental results.

Some future research directions include 1) improvement of the system performance by using less conservative consensus and device–VO coupling schemes (e.g., PSPM [9]) instead of the current (time-invariant) PD-type consensus control, 2) reduction of the amount of data for the VO consensus without compromising human perception (e.g., perception-based data reduction [45]), and 3) application of the result to more complex and practically important scenarios and investigate the issue of human perception therein (e.g., collaborative virtual surgical training).

APPENDIX

We first show the N -port consensus controller passivity (14). For this, let us denote the energy generated from the N consen-

sus control ports $(\tau_i(k), \hat{v}_i(k))$ during the k th time step by

$$\begin{aligned} s_E(k) &:= \sum_{i=1}^N \hat{v}_i^T(k) \tau_i(k) T_i^k \\ &= - \sum_{i=1}^N \left[\Lambda_i(k) + \sum_{j \in \mathcal{N}_i} \hat{v}_i^T(k) D_{ij} (\hat{v}_i(k) - \delta_{ij}^k \hat{v}_j(k - N_{ij}^k)) T_i^k \right. \\ &\quad \left. + \sum_{j \in \mathcal{N}_i} \hat{v}_i^T(k) P_{ij} (\hat{x}_i(k) - \hat{x}_j(k - N_{ij}^k)) T_i^k \right] \\ &= - \sum_{i=1}^N \Lambda_i(k) - \sum_{l=1}^{N_e} \hat{v}_p^T(k) D_{pq} [\hat{v}_p(k) - \delta_{pq}^k \hat{v}_q(k - N_{pq}^k)] T_p^k \\ &\quad - \sum_{l=1}^{N_e} \hat{v}_p^T(k) P_{pq} [\hat{x}_p(k) - \hat{x}_q(k - N_{pq}^k)] T_p^k \end{aligned}$$

where we use the fact (1) with $l \approx (p, q)$ and $\Lambda_i(k) := \|\hat{v}_i(k)\|_{B_i}^2 T_i^k$. Here, the last term, which is related to P_{pq} , can be rewritten as

$$\begin{aligned} &\sum_{l=1}^{N_e} \hat{v}_p^T(k) P_{pq} [\hat{x}_p(k) - \hat{x}_q(k)] T_p^k \\ &\quad + \sum_{l=1}^{N_e} \hat{v}_p^T(k) P_{pq} [\hat{x}_q(k) - \hat{x}_p(k - N_{pq}^k)] T_p^k \\ &= \frac{1}{2} \sum_{l=1}^{N_e} (\hat{v}_p(k) T_p^k - \hat{v}_q(k) T_q^k)^T P_{pq} (\hat{x}_p(k) - \hat{x}_q(k)) \\ &\quad + \sum_{l=1}^{N_e} \hat{v}_p^T(k) P_{pq} [\hat{x}_q(k) - \hat{x}_p(k - N_{pq}^k)] T_p^k \end{aligned}$$

where we use the fact (2) over the undirected $\mathcal{G}(\mathcal{V}, \mathcal{E})$.

Define the relative distance $\Delta x_{pq}^k := x_p(k) - x_q(k)$ and the half of the energy stored in P_{pq} on e_{pq} , $\varphi_{pq}(k) := \frac{1}{4} \|\Delta x_{pq}^k\|_{P_{pq}}^2$. Then, using the following derivation:

$$\begin{aligned} &(\hat{v}_p(k) T_p^k - \hat{v}_q(k) T_q^k)^T P_{pq} (\hat{x}_p(k) - \hat{x}_q(k)) \\ &= \frac{1}{2} (\Delta x_{pq}^{k+1} - \Delta x_{pq}^k)^T P_{pq} (\Delta x_{pq}^{k+1} + \Delta x_{pq}^k) \\ &= 2(\varphi_{pq}(k+1) - \varphi_{pq}(k)) \end{aligned}$$

we can further rewrite $s_E(k)$ s.t.

$$\begin{aligned} s_E(k) &= - \sum_{i=1}^N \underbrace{\Lambda_i(k)}_{B_i\text{-dissipation}} - \sum_{l=1}^{N_e} \underbrace{[\varphi_{pq}(k+1) - \varphi_{pq}(k)]}_{\text{energy stored in } P_{pq}} \\ &\quad - \sum_{l=1}^{N_e} \underbrace{\hat{v}_p^T(k) P_{pq} [\hat{x}_q(k) - \hat{x}_p(k - N_{pq}^k)] T_p^k}_{\text{energy generated by P-action}} \\ &\quad - \sum_{l=1}^{N_e} \underbrace{\hat{v}_p^T(k) D_{pq} [\hat{v}_p(k) - \delta_{pq}^k \hat{v}_q(k - N_{pq}^k)] T_p^k}_{\text{energy generated by D-action}} \quad (28) \end{aligned}$$

with $(p, q) \approx l$, where the first and second terms are always passivity enforcing, while the third and fourth terms may violate passivity due to the Internet's communication unreliability.

We will now show that, under condition (18), those (possibly) passivity-breaking energy generation due to the P and D actions are guaranteed to be dissipated by the local damping injection B_i , thereby, the consensus controller passivity (14) and the closed-loop passivity (13) are achieved. For this, we first obtain the upper bound of the energy generation by the P action and that of the D action, and show that the lower bound of the damping dissipation is larger than their sum under condition (18).

1) *Terms related to delayed P-action:* From (28), define

$$\Theta_{pq}(k) := \hat{v}_p^T(k) P_{pq} [\hat{x}_q(k) - \hat{x}_q(k - N_{pq}^k)] T_p^k \quad (29)$$

associated with the energy generation by the P action on the edge e_l with $(p, q) \approx l$ during the k th time index. Inserting ‘‘telescopic’’ term, $\sum_{j=k+1-N_{pq}^k}^{k-1} [\hat{x}_q(j) - \hat{x}_q(j)]$, between $\hat{x}_q(k)$ and $\hat{x}_q(k - N_{pq}^k)$, we can write $\Theta_{pq}(k)$ as

$$\begin{aligned} \Theta_{pq}(k) &= \hat{v}_p^T(k) P_{pq} \sum_{j=k-N_{pq}^k}^{k-1} [\hat{x}_q(j+1) - \hat{x}_q(j)] T_p^k \\ &= T_p^k \hat{v}_p^T(k) P_{pq} \sum_{j=k-N_{pq}^k}^{k-1} \frac{1}{2} [\hat{v}_q(j+1) T_q^{j+1} + \hat{v}_q(j) T_q^j] \\ &= T_p^k \hat{v}_p^T(k) P_{pq} \sum_{j=k+1-N_{pq}^k}^{k-1} \hat{v}_q(j) T_q^j \\ &\quad + \frac{1}{2} T_p^k \hat{v}_p^T(k) P_{pq} [\hat{v}_q(k) T_q^k + \hat{v}_q(k - N_{pq}^k) T_q^{k-N_{pq}^k}] \end{aligned}$$

where the second equality is obtained by using (9), and the third equality by combining the last two terms of the second line. Here, we set any summation $\sum_{j=k_1}^{k_2} \star_j = 0$ whenever $k_1 > k_2$. In addition, if $N_{pq}^k = 0$, we have $\Theta_{pq}(k) = 0$ in (29), trivially (and conservatively) satisfying the target inequality below (31).

Since P_{pq} is symmetric and positive definite, we have the following fact:

$$|x^T P_{pq} y| \leq \frac{1}{2} (\|x\|_{P_{pq}}^2 + \|y\|_{P_{pq}}^2) \quad (30)$$

for any $x, y \in \mathfrak{R}^n$. Using this, we can then show that

$$\begin{aligned} |\Theta_{pq}(k)| &\leq \frac{1}{2} T_p^k \sum_{j=k+1-N_{pq}^k}^{k-1} T_q^j [\|\hat{v}_p(k)\|_{P_{pq}}^2 + \|\hat{v}_q(j)\|_{P_{pq}}^2] \\ &\quad + \frac{1}{4} T_p^k T_q^k [\|\hat{v}_p(k)\|_{P_{pq}}^2 + \|\hat{v}_q(k)\|_{P_{pq}}^2] \\ &\quad + \frac{1}{4} T_p^k T_q^{k-N_{pq}^k} [\|\hat{v}_p(k)\|_{P_{pq}}^2 + \|\hat{v}_q(k - N_{pq}^k)\|_{P_{pq}}^2] \\ &= \frac{1}{4} \alpha_{pq}(k) \left[\sum_{j=k-N_{pq}^k}^{k-1} T_q^j + \sum_{j=k-N_{pq}^k+1}^k T_q^j \right] \end{aligned}$$

$$+ \frac{1}{4} T_p^k \left[\sum_{j=k-N_{pq}^k}^{k-1} \alpha_{qp}(j) + \sum_{j=k-N_{pq}^k+1}^k \alpha_{qp}(j) \right]$$

with $\alpha_{pq}(k) := T_p^k \|\hat{v}_p(k)\|_{P_{pq}}^2 \geq 0$, where the equality is obtained by splitting the two terms in the first line and combining them with the remaining terms.

Since $\mathcal{G}(\mathcal{V}, \mathcal{E})$ is undirected with $P_{pq} = P_{qp}$, we can also define $\Theta_{qp}(k)$ and obtain $|\Theta_{qp}(k)|$ similar to earlier, with p and q swapped with each other. Summing them up and collecting the terms containing α_{pq} and α_{qp} separately, we can show that

$$|\Theta_{pq}(k)| + |\Theta_{qp}(k)| \leq \Omega_{pq}(k) + \Omega_{qp}(k) \quad (31)$$

where

$$\begin{aligned} \Omega_{pq}(k) &:= \frac{1}{4} \alpha_{pq}(k) \left[\sum_{j=k-N_{pq}^k}^{k-1} T_q^j + \sum_{j=k-N_{pq}^k+1}^k T_q^j \right] \\ &\quad + \frac{1}{4} T_q^k \left[\sum_{j=k-N_{qp}^k}^{k-1} \alpha_{pq}(j) + \sum_{j=k-N_{qp}^k+1}^k \alpha_{pq}(j) \right] \\ &\leq \frac{1}{4} T_q^{\max} \left[2\bar{N}_{pq} \alpha_{pq}(k) + \sum_{j=k-\bar{N}_{qp}}^{k-1} \alpha_{pq}(j) + \sum_{j=k-\bar{N}_{qp}+1}^k \alpha_{pq}(j) \right]. \end{aligned}$$

Then, by summing $\Omega_{pq}(k)$ over the time, we have

$$\begin{aligned} \sum_{k=0}^{\bar{M}} \Omega_{pq}(k) &\leq \frac{T_q^{\max}}{2} \sum_{k=0}^{\bar{M}} \left[\bar{N}_{pq} \alpha_{pq}(k) + \sum_{j=k-\bar{N}_{qp}+1}^k \alpha_{pq}(j) \right] \\ &= \sum_{k=0}^{\bar{M}} \frac{\bar{N}_{pq} + \bar{N}_{qp}}{2} T_q^{\max} \alpha_{pq}(k) \\ &\quad - \frac{T_q^{\max}}{2} \sum_{k=1}^{\bar{N}_{qp}-1} k \alpha_{pq}(k + \bar{M} - \bar{N}_{qp} + 1) \\ &\leq \sum_{k=0}^{\bar{M}} \frac{\bar{N}_{pq} + \bar{N}_{qp}}{2} T_q^{\max} \alpha_{pq}(k) \quad (32) \end{aligned}$$

where the first inequality is because

$$\begin{aligned} \sum_{k=0}^{\bar{M}} \left[\sum_{j=k-\bar{N}_{qp}}^{k-1} \alpha_{pq}(j) + \sum_{j=k-\bar{N}_{qp}+1}^k \alpha_{pq}(j) \right] \\ = \sum_{k=0}^{\bar{M}} \left[2 \sum_{j=k-\bar{N}_{qp}+1}^k \alpha_{pq}(j) + \alpha_{pq}(k - \bar{N}_{qp}) - \alpha_{pq}(k) \right] \\ = 2 \sum_{k=0}^{\bar{M}} \sum_{j=k-\bar{N}_{qp}+1}^k \alpha_{pq}(j) + \sum_{k=0}^{\bar{M}} [\alpha_{pq}(k - \bar{N}_{qp}) - \alpha_{pq}(k)] \end{aligned}$$

where the last term is always negative, since $\alpha_{pq}(k) \geq 0$ with $\alpha_{pq}(k) = 0$ for $k < 0$. The last inequality of (32) is also because $\alpha_{pq}(k) \geq 0$. On the other hand, the equality in the second line

of (32) is from the fact that

$$\begin{aligned} & \sum_{k=0}^{\bar{M}} \sum_{j=k-\bar{N}_{qp}+1}^k \alpha_{pq}(j) \\ &= \sum_{k=0}^{\bar{M}} \bar{N}_{qp} \alpha_{pq}(k) - \sum_{k=1}^{\bar{N}_{qp}-1} k \alpha_{pq}(\bar{M} - \bar{N}_{qp} + 1 + k) \end{aligned} \quad (33)$$

which can be shown as follows: 1) Write k from 0 to \bar{M} horizontally and each term of $\sum_{j=k-\bar{N}_{qp}+1}^k \alpha_{pq}(j)$ top down from $j = k - \bar{N}_{qp} + 1$ to $j = k$ with $\alpha_{qp}(k) = 0$ for $k < 0$ [i.e., all the terms in the left-hand side of (33)]; 2) append them with terms to collectively make a parallelogram shape with its top and bottom lines, respectively, consisting of $\bar{N}_{qp} \alpha_{pq}(0)$ and $\alpha_{pq}(\bar{M})$; 3) add all the terms in this parallelogram [i.e., first term in (33)]; and 4) subtract the terms that were added to make the parallelogram [i.e., second term in (33)].

2) *Terms related to delayed D-action:* This energy can be written as follows. For the edge $e_l \in \mathcal{E}$ with $(p, q) \approx l$, we have

$$\begin{aligned} \Upsilon_{pq}(k) &:= \hat{v}_p^T(k) D_{pq} [\hat{v}_p(k) - \delta_{pq}^k \hat{v}_p(k - N_{pq}^k)] T_p^k \\ &\geq \|\hat{v}_p(k)\|_{D_{pq} T_p}^2 \\ &\quad - \frac{1}{2} \delta_{pq}^k (\|\hat{v}_p(k)\|_{D_{pq}}^2 + \|\hat{v}_q(k - N_{pq}^k)\|_{D_{pq}}^2) T_p^k \\ &\geq \frac{1}{2} (\|\hat{v}_p(k)\|_{D_{pq} T_p}^2 - \delta_{pq}^k \|\hat{v}_q(k - N_{pq}^k)\|_{D_{pq} T_p}^2) \end{aligned} \quad (34)$$

where we use (30) and the fact that $\delta_{pq}^k = \{0, 1\}$. Then, similar to (31), since the graph $\mathcal{G}(\mathcal{V}, \mathcal{E})$ is undirected with $D_{pq} = D_{qp}$, we can obtain inequality similar to the above for Υ_{qp} . Further, combining those for Υ_{pq} and Υ_{qp} , we can have

$$\Upsilon_{pq}(k) + \Upsilon_{qp}(k) \geq \Psi_{pq}(k) + \Psi_{qp}(k) \quad (35)$$

where

$$\Psi_{pq}(k) := \frac{1}{2} (\|\hat{v}_p(k)\|_{D_{pq} T_p}^2 - \delta_{qp}^k \|\hat{v}_p(k - N_{qp}^k)\|_{D_{pq} T_q}^2).$$

Summing this $\Psi_{pq}(k)$ over time then yields

$$\begin{aligned} & \sum_{k=0}^{\bar{M}} \Psi_{pq}(k) \\ &\geq \frac{1}{2} \sum_{k=0}^{\bar{M}} (\|\hat{v}_p(k)\|_{D_{pq} T_p}^{\min} - \delta_{qp}^k \|\hat{v}_p(k - N_{qp}^k)\|_{D_{pq} T_q}^{\max}) \\ &\geq \frac{1}{2} \sum_{k=0}^{\bar{M}} (\|\hat{v}_p(k)\|_{D_{pq} T_p}^{\min} - \delta_{qp}^k \|\hat{v}_p(k)\|_{D_{pq} T_q}^{\max}) \\ &\geq \frac{1}{2} \sum_{k=0}^{\bar{M}} (T_p^{\min} - T_q^{\max}) \|\hat{v}_p(k)\|_{D_{pq}}^2 \end{aligned} \quad (36)$$

where the first inequality is from the definition of T_p^{\min}, T_q^{\max} , while the second and third inequalities are because $\delta_{qp}^k \in \{0, 1\}$ and no data duplication with this δ_{qp}^k (17), and $\|\hat{v}_p(k)\|_{D_{pq}}^2 \geq 0$, with $\|\hat{v}_p(k)\|_{D_{pq}}^2 = 0$ for $k < 0$.

Now, we prove the N -port consensus controller passivity (14) under condition (18). First, using (18), we can compute a lower bound for the energy dissipation by the local damping B_i s.t.

$$\begin{aligned} & \sum_{k=0}^{\bar{M}} \sum_{i=1}^N \|\hat{v}_i(k)\|_{B_i T_i}^2 \\ &\geq \sum_{k=0}^{\bar{M}} \sum_{i=1}^N \sum_{j \in N_i} \left(\frac{\bar{N}_{ij} + \bar{N}_{ji}}{2} T_j^{\max} \|\hat{v}_i(k)\|_{K_{ij} T_i}^2 \right. \\ &\quad \left. + \frac{1}{2} \left[\frac{T_j^{\max}}{T_i^{\min}} - 1 \right] T_i^k \|\hat{v}_i(k)\|_{D_{ij}}^2 \right) \\ &\geq \sum_{k=0}^{\bar{M}} \sum_{l=1}^{N_e} \left(\frac{\bar{N}_{pq} + \bar{N}_{pq}}{2} T_q^{\max} \alpha_{pq}(k) \right. \\ &\quad \left. + \frac{1}{2} [T_q^{\max} - T_p^{\min}] \|\hat{v}_p(k)\|_{D_{pq}}^2 \right) \end{aligned} \quad (37)$$

where $(p, q) \approx l$, $\alpha_{pq}(k) := \|\hat{v}_p(k)\|_{D_{pq} T_p}^2$, and the second inequality is due to the fact 1 and $T_p^k / T_p^{\min} \geq 1$.

Then, from (28) using (29) and (34), along with (31), (32), (35), and (36), we can achieve the N -port controller passivity (14), i.e., $\forall \bar{M} \geq 0$

$$\begin{aligned} \sum_{k=0}^{\bar{M}} s_E(k) &= - \sum_{k=0}^{\bar{M}} \sum_{i=1}^N \Lambda_i(k) + \sum_{l=1}^{N_e} [\varphi_{pq}(0) - \varphi_{pq}(\bar{M} + 1)] \\ &\quad - \sum_{k=0}^{\bar{M}} \sum_{l=1}^{N_e} \Theta_{pq}(k) - \sum_{k=0}^{\bar{M}} \sum_{l=1}^{N_e} \Upsilon_{pq}(k) \\ &\leq \sum_{l=1}^{N_e} \varphi_{pq}(0) =: c^2 \end{aligned} \quad (38)$$

where, for the inequality, we also use the fact that

$$- \sum_{k=0}^{\bar{M}} \sum_{l=1}^{N_e} \Theta_{pq}(k) \leq \sum_{k=0}^{\bar{M}} \sum_{l=1}^{N_e} |\Theta_{pq}(k)| \leq \sum_{k=0}^{\bar{M}} \sum_{l=1}^{N_e} \Omega_{pq}(k).$$

REFERENCES

- [1] D. J. Lee and K. Huang, "Peer-to-peer control architecture for multiuser haptic collaboration over undirected delayed packet-switching network," in *Proc. IEEE Int. Conf. Robot. Autom.*, May 2010, pp. 1333–1338.
- [2] K. Huang and D. J. Lee, "Passivity-based position consensus of multiple mechanical integrators with communication delay," in *Proc. Amer. Control Conf.*, 2010, pp. 836–841.
- [3] K. Huang and D. J. Lee, "Hybrid virtual-proxy based control framework for passive bilateral teleoperation over the Internet," in *Proc. IEEE/RSJ Int. Conf. Intell. Robot. Syst.*, Sep. 2011, pp. 149–156.
- [4] H. Delingette, "Toward realistic soft-tissue modeling in medical simulation," *Proc. IEEE*, vol. 86, no. 3, pp. 512–523, Mar. 1998.
- [5] D. J. Lee and K. Huang, "On passive non-iterative varying-step numerical integration of mechanical systems for haptic rendering," in *Proc. ASME Dynam. Syst. Control Conf.*, 2008, pp. 1147–1154.
- [6] D. J. Lee, M. Kim, and T. Qiu, "Passive haptic rendering and control of Lagrangian virtual proxy," in *Proc. IEEE/RSJ Int. Conf. Intell. Robot. Syst.*, 2012, pp. 64–69.
- [7] J. E. Colgate, M. C. Stanley, and J. M. Brown, "Issues in the haptic display of tool use," in *Proc. IEEE/RSJ Int. Conf. Intell. Robot. Syst.*, Aug. 1995, vol. 3, pp. 140–145.

- [8] D. J. Lee, "Extension of colgate's passivity condition for variable-rate haptics," in *Proc. IEEE/RSJ Int. Conf. Intell. Robot. Syst.*, Oct. 2009, pp. 1761–1766.
- [9] D. J. Lee and K. Huang, "Passive-set-position-modulation framework for interactive robotic systems," *IEEE Trans. Robot.*, vol. 26, no. 2, pp. 354–369, Apr. 2010.
- [10] N. Hogan, "Controlling impedance at the man/machine interface," in *Proc. IEEE Int. Conf. Robot. Autom.*, May 1989, vol. 3, pp. 1626–1631.
- [11] M. W. Spong, S. Hutchinson, and M. Vidyasagar, *Robot Modeling and Control*. New York: Wiley, 2006.
- [12] J. M. Brown and J. E. Colgate, "Passive implementation of multibody simulations for haptic display," in *Proc. ASME Int. Mech. Eng. Congr. Exhib.*, 1997, pp. 85–92.
- [13] J. M. Brown and J. E. Colgate, "Minimum mass for haptic display simulations," in *Proc. ASME Int. Mech. Eng. Congr. Expo.*, 1998, pp. 249–256.
- [14] P. Buttolo, R. Oboe, and B. Hannaford, "Architectures for shared haptic virtual environments," *Comput. Graph.*, vol. 21, no. 4, pp. 421–429, 1997.
- [15] J. P. Hespanha, M. McLaughlin, G. S. Sukhatme, M. Akbarian, R. Garg, and W. Zhu, "Haptic collaboration over the Internet," presented at the 5th Phantom Users Group Workshop, Aspen, CO, 2000.
- [16] J. Kim, H. Kim, B. K. Tay, M. Muniyandi, M. A. Srinivasan, J. Jordan, J. Mortensen, M. Oliveira, and M. Slater, "Transatlantic touch: A study of haptic collaboration over long distance," in *Presence: Teleoperators & Virtual Environments*, vol. 13. Cambridge, MA: MIT Press, 2004, pp. 328–337.
- [17] X. J. Shen, J. L. Zhou, A. El Saddik, and N. D. Georganas, "Architecture and evaluation of tele-haptic environments," in *Proc. IEEE Int. Symp. Distrib. Simul. Real-Time Appl.*, Oct. 2004, pp. 53–60.
- [18] O. Wongwirat and S. Ohara, "Haptic media synchronization for remote surgery through simulation," *IEEE Multimedia*, vol. 13, no. 3, pp. 62–69, Jul. 2006.
- [19] G. Sankaranarayanan and B. Hannaford, "Experimental Internet haptic collaboration using virtual coupling schemes," in *Proc. Symp. Haptic Interfaces Virtual Environ. Teleoperator Syst.*, 2008, pp. 259–266.
- [20] G. Sankaranarayanan and B. Hannaford, "Virtual coupling schemes for position coherency in networked haptic environments," in *Proc. IEEE/RAS-EMBS Int. Conf. Biomed. Robot. Biomechatron.*, Feb. 2006, pp. 853–858.
- [21] Z. Li and D. Constantinescu, "Remote dynamic proxies for wave-based peer-to-peer haptic interaction," in *Proc. Joint Eur. Conf. Haptic Symp.*, 2009, pp. 553–558.
- [22] M. Fotoohi, S. Sirouspour, and D. Capson, "Stability and performance analysis of centralized and distributed multi-rate control architectures for multi-user haptic interaction," *Int. J. Robot. Res.*, vol. 26, no. 9, pp. 977–994, 2007.
- [23] J. Cheong, S.-I. Niculescu, and C. Kim, "Motion synchronization control of distributed multisubsystems with invariant local natural dynamics," *IEEE Trans. Robot.*, vol. 25, no. 2, pp. 382–398, Apr. 2009.
- [24] T. Hayakawa, T. Matsuzawa, and S. Hara, "Formation control of multi-agent systems with sampled information," in *Proc. IEEE Conf. Decision Control*, Dec. 2006, pp. 4333–4338.
- [25] W. Ren and Y. C. Cao, "Convergence of sampled-data consensus algorithms for double-integrator dynamics," in *Proc. IEEE Conf. Decision Control*, Dec. 2008, pp. 3965–3970.
- [26] P. Lin and Y. M. Jia, "Consensus of second-order discrete-time multi-agent systems with nonuniform time-delays and dynamically changing topologies," *Automatica*, vol. 45, no. 9, pp. 2154–2158, 2009.
- [27] R. Olfati-Saber and R. M. Murray, "Consensus problems in networks of agents with switching topology and time-delays," *IEEE Trans. Autom. Control*, vol. 49, no. 9, pp. 1520–1533, Sep. 2004.
- [28] W. Ren and R. W. Beard, "Consensus seeking in multiagent systems under dynamically changing interaction topologies," *IEEE Trans. Autom. Control*, vol. 50, no. 5, pp. 655–661, May 2005.
- [29] D. J. Lee and M. W. Spong, "Stable flocking of multiple inertial agents on balanced graphs," *IEEE Trans. Autom. Control*, vol. 52, no. 8, pp. 1469–1475, Aug. 2007.
- [30] N. Biggs, *Algebraic Graph Theory*, 2nd ed. Cambridge, U.K.: Cambridge Univ. Press, 1993.
- [31] P. Y. Li, "Coordinated contour following control for machining operations—A survey," in *Proc. Amer. Control Conf.*, 1999, pp. 4543–4547.
- [32] P. Ogren, E. Fiorelli, and N. E. Leonard, "Cooperative control of mobile sensor networks: Adaptive gradient climbing in a distributed environment," *IEEE Trans. Autom. Control*, vol. 49, no. 8, pp. 1292–1302, Aug. 2004.
- [33] T. J. R. Hughes, *The Finite Element Method: Linear Static and Dynamic Finite Element Analysis*. Mineola, NY: Dover, 2000.
- [34] D. J. Lee and P. Y. Li, "Passive bilateral control and tool dynamics rendering for nonlinear mechanical teleoperators," *IEEE Trans. Robot.*, vol. 21, no. 5, pp. 936–951, Oct. 2005.
- [35] D. J. Lee and M. W. Spong, "Passive bilateral teleoperation with constant time delay," *IEEE Trans. Robot.*, vol. 22, no. 2, pp. 269–281, Apr. 2006.
- [36] S. Boyd, P. Diaconis, and L. Xiao, "Fastest mixing Markov chain on a graph," *SIAM Rev.*, vol. 46, no. 4, pp. 667–689, 2004.
- [37] Y. Kim and M. Mesbahi, "On maximizing the second smallest eigenvalue of a state-dependent graph Laplacian," *IEEE Trans. Autom. Control*, vol. 51, no. 1, pp. 116–120, Jan. 2006.
- [38] M. V. Marathe, R. Ravi, R. Sundaram, S. S. Ravi, D. J. Rosenkrantz, and H. B. Hunt III, "Bicriteria network design problems," *J. Algorithms*, vol. 28, pp. 142–171, 1998.
- [39] Y. Dodis and S. Khanna, "Designing networks with bounded pairwise distance," in *Proc. 31st Annu. ACM Symp. Theory Comput.*, 1999, pp. 750–759.
- [40] Y. J. Lee and M. Atiqzaman, "Least cost heuristic for the delay-constrained capacitated minimum spanning tree problem," *Comput. Commun.*, vol. 28, no. 11, pp. 1371–1379, 2005.
- [41] J.-C. Bolot, "End-to-end packet delay and loss behavior in the Internet," in *Proc. SIGCOMM*, 1993, pp. 289–298.
- [42] W. Jiang and H. Schulzrinne, "Modeling of packet loss and delay and their effect on real-time multimedia service quality," presented at the 10th Int. Workshop Netw. Operating Syst. Support Digital Audio Video, Chapel Hill, NC, 2000.
- [43] G. Niemeyer and J.-J. E. Slotine, "Telemanipulation with time delays," *Int. J. Robot. Res.*, vol. 23, no. 9, pp. 873–890, Sep. 2004.
- [44] D. P. Bertsekas and J. N. Tsitsiklis, *Parallel and Distributed Computation: Numerical Methods*. Englewood Cliffs, NJ: Prentice-Hall, 1989.
- [45] P. Hinterseer, S. Hirche, S. Chaundhuri, E. Steinbach, and M. Buss, "Perception-based data reduction and transmission of haptic data in telepresence and teleaction systems," *IEEE Trans. Signal Process.*, vol. 56, no. 2, pp. 588–597, Feb. 2008.



Ke Huang received the B.S. degree in automation from the University of Science and Technology of China, Hefei, China, in 2005 and the Ph.D. degree in mechanical engineering from the University of Tennessee, Knoxville, in 2012.

From January to June 2012, he was a Postdoctoral Research Specialist with Rensselaer Polytechnic Institute Troy, NY. Since June 2012, he has been a Principle Engineer with Western Digital Corporation, Irvine, CA. His research interests include bilateral teleoperation, multiagent distributed coordination, and multiuser haptic collaboration over the Internet.



Dongjun Lee (S'02–M'04) received the B.S. degree in mechanical engineering from the Korea Advanced Institute of Science and Technology (KAIST), Daejeon, Korea, in 1995, the M.S. degree in automation and design from KAIST, Seoul, Korea, in 1997, and the Ph.D. degree in mechanical engineering from the University of Minnesota, Twin Cities, in 2004.

Since 2011, he has been an Assistant Professor with the School of Mechanical and Aerospace Engineering, Seoul National University, Seoul, Korea. He was an Assistant Professor with the Department of

Mechanical, Aerospace, and Biomedical Engineering, University of Tennessee, Knoxville, from 2006 to 2011; a Postdoctoral Research Fellow with the Coordinated Science Laboratory, University of Illinois at Urbana-Champaign from 2004 to 2006; and an Engine Development Engineer with Kia Motors Corporation, Seoul, Korea, from 1997 to 1999. He was a Doctoral Dissertation Fellow with the University of Minnesota from 2002 to 2003. His main research interests include dynamics and control of robotic and mechatronic systems with particular emphasis on teleoperation/haptics, multirobot systems, nonholonomic systems, aerial robotics, and geometric mechanics control theory.

Dr. Lee received the U.S. National Science Foundation CAREER Award in 2009, the Best Paper Award from the International Conference on Intelligent Autonomous Systems in 2012, and was a 2002–2003 Doctoral Dissertation Fellow of the University of Minnesota.